HUMAN PILOT DYNAMIC RESPONSE IN SINGLE-LOOP SYSTEMS WITH COMPENSATORY AND PURSUIT DISPLAYS

R. J. Wasicko
D. T. McRuer
R. E. Magdaleno

SYSTEMS TECHNOLOGY, INC.

TECHNICAL REPORT AFFDL-TR-66-137

December 1966

AIR FORCE FLIGHT DYNAMICS LABORATORY
RESEARCH AND TECHNOLOGY DIVISION
AIR FORCE SYSTEMS COMMAND

WRIGHT-PATTERSON AIR FORCE BASE, OHIO

NOTICES

When Government drawings, specifications, or other data are used for any purpose other than in connection with a definitely related Government procurement operation, the United States Government thereby incurs no responsibility nor any obligation whatsoever, and the fact that the Government may have formulated, furnished, or in any way supplied the said drawings, specifications, or other data, is not to be regarded by implication or otherwise as in any manner licensing the holder or any other person or corporation, or conveying any rights or permission to manufacture, use, or sell any patented invention that may in any way be related thereto.

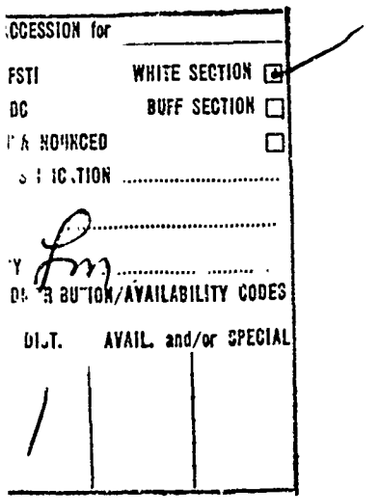

Copies of this report should not be returned to the Research and Technology Division unless return is required by security considerations, contractual obligations, or notice on a specific document.

AFFDL-TR-66-137

HUMAN PILOT DYNAMIC RESPONSE IN SINGLE-LOOP SYSTEMS WITH COMPENSATORY AND PURSUIT DISPLAYS

R. J. Wasicko
D. T. McRuer
R. E. Magdaleno

ERRATA

The data plots and controlled element designations on p. 29 should be interchanged with that on p. 52.

FOREWORD

This report documents an analytical and experimental investigation of human pilot dynamics accomplished under Contract AF 33(657)-10835, BPS No. 5(6399-8219-62405364), sponsored by the Flight Control Division of the Air Force Flight Dynamics Laboratory. The research was performed by Systems Technology, Inc., at both its Hawthorne, California, and Princeton, New Jersey, offices, and, under subcontract, by The Franklin Institute Laboratories, Philadelphia, Pennsylvania. The project principal investigators were D. T. McRuer and D. Graham, of STI, and E. S. Krendel, of FIL. The Flight Control Division project engineers were Capt. J. E. Pruner and P. E. Pietrzak.

Many others besides the authors have contributed to the results reported here. All of the principal investigators participated in the detailed planning phases. An important contribution was made by William C. Reisener, Jr., of The Franklin Institute, who executed the experiments and data reduction phases. The authors would also like to thank their co-workers M. M. Solow, who was the subject, and Diane Fackenthal, who assisted in the data reduction phase; and A. V. Phatak, of STI, who assisted in pre-experiment calculations and predictions. Finally, the report has been significantly improved by the incorporation of many suggestions due to the careful review by R. O. Anderson and P. E. Pietrzak of FDCC. This manuscript was released by the authors in December 1966 for publication as an RTD Technical Report.

This technical report has been reviewed and is approved.

C. B. WESTBROOK
Chief, Control Criteria Branch
Flight Control Division
AF Flight Dynamics Laboratory

ABSTRACT

The primary purpose of the experimental series reported here is to investigate, on a preliminary and exploratory basis, human operator performance differences between pursuit and compensatory displays. For each display type a wide range of forcing function bandwidths and controlled element dynamics was used. The effect of the additional information provided by separately displaying both forcing function and controlled element output (pursuit) rather than their difference (compensatory) was evaluated using the mean-squared error and a quantity called the "effective open-loop describing function" (Y_β).

As a prelude to the new data, past pursuit/compensatory tracking results are reviewed, and then a tie-in is made between these and the current series.

TABLE OF CONTENTS

ILLUSTRATIONS

TABLES

SYMBOLS

B5	Forcing function designation defined on page 18
c,c(t)	Human operator output
c_i	Portion of human operator output that is linearly correlated with forcing function
c_n	Portion of human operator output that is not linearly correlated with forcing function
C	Compensatory display
C	Fourier transform of c(t)
d(t)	Second input defined on page 16
e(t)	Operator stimulus; error
e_i	Portion of error that is linearly correlated with forcing function
e_n	Portion of error that is not linearly correlated with forcing function
E	Fourier transform of e(t)
F_s	Stick force gradient
i(t)	System forcing function
I	Fourier transform of i(t)
$j\omega$	Imaginary part of the complex variable, $s = \sigma \pm j\omega$
K_c	Controlled element gain
K_s	Control sensitivity — inches (display)/stick motion
m(t)	System output
M	Fourier transform of m(t)
n_{ω}	$T_R\omega_n/2\pi$ defined on page 20
$n_c(t)$	Remnant injected at pilot's output
N	Number of runs

N_c	Fourier transform of n_c
P	Pursuit display
R.24	Ref. 3 forcing function designation defined on page 41
R.4	Ref. 3 forcing function designation defined on page 41
R.64	Ref. 3 forcing function designation defined on page 41
R14	Forcing function designation defined on page 18
s	Laplace transform variable, $s = \sigma \pm j\omega$
t	Time
T_R	Run length
Y_c	Controlled element
Y_{p_c}	Human operator describing function with compensatory display
Y_{p_e}	Human operator describing function operating on e(t) (Pursuit display)
Y_{p_i}	Human operator describing function operating on i(t) (Pursuit display)
$Y_{p_i}^*$	Implied Y_{p_i} on assumption that $Y_{p_e} = Y_{p_c}$ and $Y_{p_m} = 0$
Y_{p_m}	Human operator describing function operating on m(t) (Pursuit display)
Y_β	Effective open-loop describing function
λ	Controlled element parameter
σ_e	rms value of the error
σ_i	rms value of the forcing function
φ_i	Peak amplitude of an input sine wave
Φ_{dc}	Cross spectral density between d and c
Φ_{de}	Cross spectral density between d and e
Φ_{ee}	Error spectral density
Φ_{ic}	Cross power spectral density between i and c
Φ_{ie}	Cross power spectral density between i and e

Φ_{ii}	Forcing function power spectral density
Φ_{im}	Cross spectral density between i and m
Φ_{mm}	System output power spectral density
$\Phi_{n_c c}$	Cross spectral density between n_c and c
$\Phi_{n_c e}$	Cross spectral density between n_c and e
$\Phi_{n_c m}$	Cross spectral density between n_c and m
Φ_{nn}	Closed-loop remnant spectral density, at pilot's output
$\Phi_{n_c n_c}$	Power spectral density of n_c
ω	Angular frequency, rad/sec
ω_c	System crossover frequency, i.e., frequency at which $\lvert Y_p Y_c \rvert = 1$
ω_{c_β}	Crossover frequency of Y_β
ω_i	Forcing function bandwidth
ω_n	Frequency of the "nth" sinusoidal component of the forcing function
$\doteq$	Approximately equal to
$\measuredangle$	Angle of
db	Decibels; 10 $\log_{10}$ if a power quantity, e.g., spectrum; 20 $\log_{10}$ if an amplitude quantity, e.g., Y_p
$\lvert\ \rvert$	Magnitude
$\lvert\ \rvert_{db}$	Magnitude in db
$\bar{(\ )}$	Mean value ensemble average
$\mathcal{L}^{-1}$	Inverse Laplace transform

CHAPTER I

INTRODUCTION

A. BACKGROUND AND MOTIVATION

The usefulness of a control engineering approach to the study and design of manual vehicular control systems has grown rapidly in the past decade and is now well established. This approach requires models of pilot dynamic characteristics which can be applied in conjunction with the formal methods of control engineering. The models are based on experimental measurements of dynamic characteristics exhibited by pilots in a variety of control situations. A great many past experiments in which human dynamic measurements were taken have considered so-called compensatory conditions, i.e., those in which the operator's actions are based solely on an error indicating the difference between system command and system output (Fig. 1a). In contrast, the more complex pursuit situation, i.e., that in which the system forcing function and output are displayed to the operator and he can utilize both, and/or their difference (system error) as his basis for control action, has received very little attention (Fig. 1b). In fact, the only experiments in which human operator dynamics have been obtained are those of Ref. 3. While this experimental series comprehensively covered effects of forcing function variations on operator dynamics, the controlled element dynamics were made the simplest possible (a pure gain, $Y_c = 1$) and were held fixed. A variety of other experiments in which performance measures only were taken (Refs. 1, 2, 9) has demonstrated the overwhelming importance of controlled element characteristics as task variables. However, the nature of the dynamic characteristics adopted by the operator which underlie the performance differences noted with different controlled elements has been unknown. In the absence of an experimental data base, the models of pilot dynamics in pursuit situations have been only conjectures. The experimental series described here was undertaken primarily to provide such data. Then, as these and other new data enhance our quantitative understanding of pursuit display systems, the next step is the evolution of a mathematical pilot model which is suitable for predictive purposes.

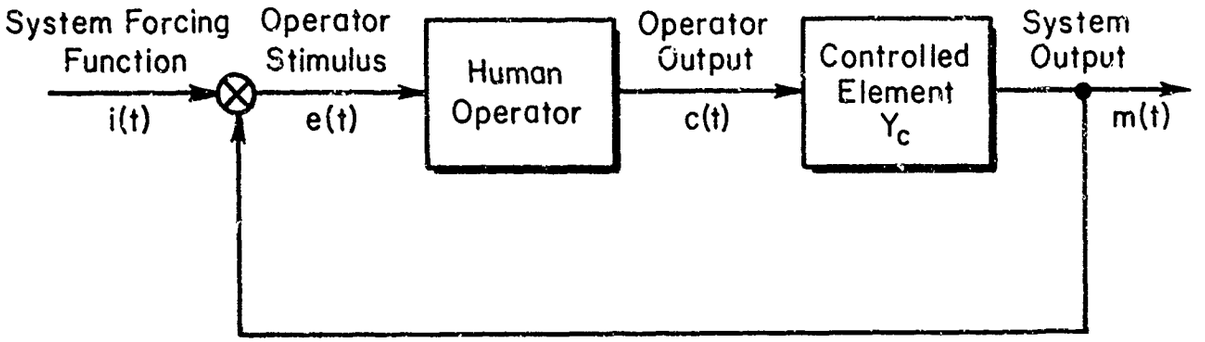

a) Functional Block Diagram for Compensatory Behavior

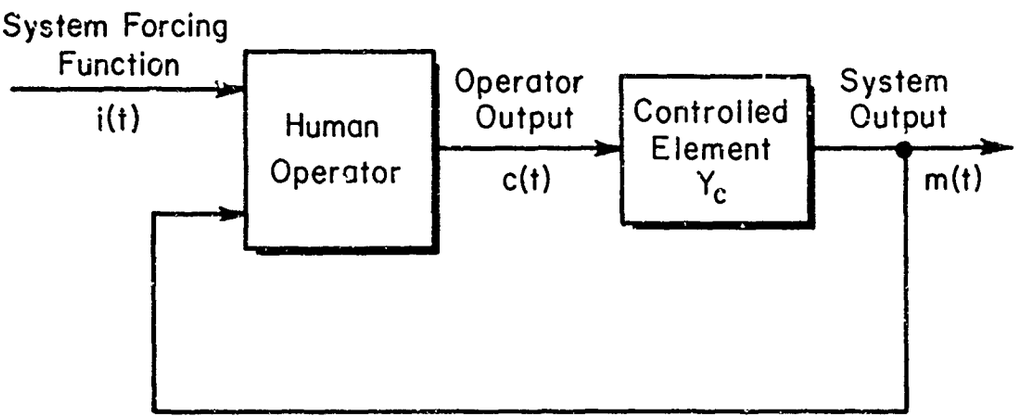

b) Functional Block Diagram for Pursuit Behavior

Figure 1. Compensatory and Pursuit Manual Control Systems

The compensatory and pursuit manual control systems indicated in Fig. 1 are intended to represent different behavioral situations. In compensatory operation only the system error acts as a stimulus for operator action, whereas in pursuit the system forcing function and output are separately observable. These two different situations are ordinarily defined in terms of pursuit and compensatory displays (Fig. 2) which actually present the appropriate system signals as visual stimuli. However, it is important to recognize that presentation of the signals does not necessarily imply pilot action thereon; for instance, in a pursuit display the operator may act only on the error, thereby performing in a compensatory fashion in spite of the presence of the forcing function and output. Conversely, under certain conditions with a compensatory display (e.g., a predictable forcing function) the operator

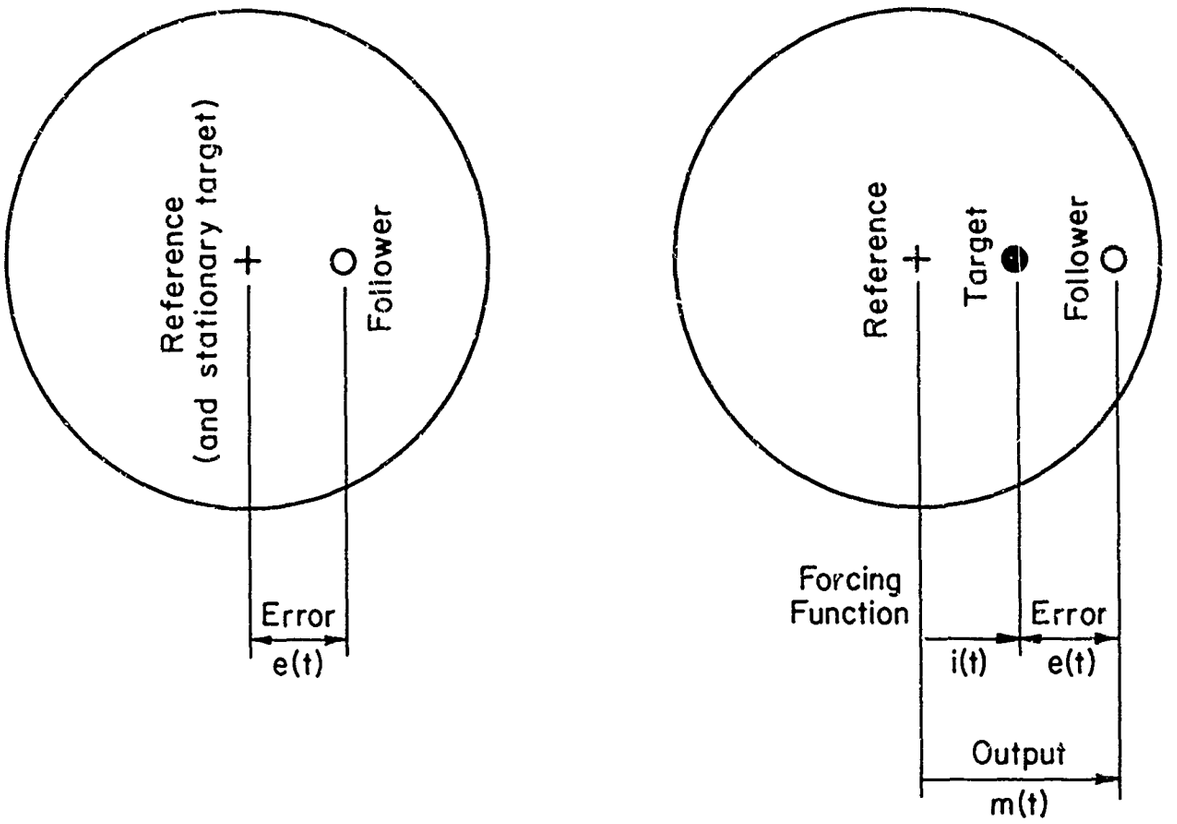

Figure 2. Compensatory and Pursuit Displays

can mentally separate input from output in the displayed error signal. Then by using a reasonable facsimile of the system forcing function and the error as information inputs the operator may function in a pursuit fashion. With random-appearing inputs and complex controlled element dynamics, the usual way to induce compensatory or pursuit behavior is by virtue of the display. This always works in the compensatory situation, although, as indicated above, the provision of a pursuit display does not guarantee pursuit operation by the operator.

There are many practical reasons for our interest in obtaining a quantitative understanding of the human operator response in pursuit situations. These include, but are not limited to, the following:

- In tasks where the external reference is present (e.g., VFR approach and landing), a pursuit model may be an appropriate representation for the human's operation.

- For director (as opposed to null steering) displays in IFR operations, the type of behavior desired and the appropriate pilot model correspond to those of the pursuit situation.
- As hypothesized by the Successive Organizations of Perception (SOP) theory (Ref. 6), a pursuit mode of response by the operator is an interim phase in the development of exceptional skill. In this hypothesis, pursuit behavior will occur both in the progression toward higher skills and in the regression to lower levels (compensatory) under stress.
- For many situations, tracking performance (rms error) with a pursuit display is superior to that for a compensatory display. Determination of a simple, usable model for operator response behavior with pursuit-like visual presentation of information (from the external field of view or displays) is required for system synthesis activities for which improved performance is desired.

B. GENERAL PLAN

The intent of the experiments reported here was to explore the nature of differences between pursuit and compensatory behavior for a wide cross section of forcing function characteristics and controlled element dynamics. To accomplish this the same forcing function and controlled element task variables were used for two different display configurations. The human pilot dynamics were characterized by describing function measurements, and the average system performance by appropriate performance measures. Differences in dynamic behavior between the two situations were detected by comparing (1) the mean-squared errors and (2) an effective open-loop describing function for the pursuit display with the actual open-loop describing function exhibited with the compensatory display. The latter provided a very sensitive measure of dynamic changes induced by the display differences. The remnant differences between the two display situations were found by examining the two components of the mean-squared error, i.e., that due to pilot/system dynamics operating on the forcing function and that due to the effects of pilot remnant operating within the closed-loop system.

C. OUTLINE OF THE REPORT

The preceding introduction indicates that the purpose of this experimental series is to study the means used by the pilot to enhance performance in pursuit systems over that in compensatory systems. A quantitative understanding is desired, preferably to the extent that a mathematical model suitable for predictive purposes is obtained.

Chapter II reviews and summarizes past pursuit/compensatory studies for later comparison with the results of the present experiments. Consideration is restricted to those previous studies that utilized random-appearing inputs which allow direct comparison with our data.

Chapter III discusses the system relationships that result from the pilot's utilization of the additional information provided by the pursuit display. Of major importance is the section "Detection of Pursuit Behavior," where it is shown that performance measures alone are inadequate. Supplementing these with an effective open-loop describing function is shown to provide sufficient information to detect pursuit behavior. This chapter concludes with a description of the experimental configuration.

Chapters II and III lead directly to the desired experimental plan given in Chapter IV. This is followed by the performance measure and describing function data, with extensive comparisons of the present subject's compensatory display data with a large population of pilots to indicate that he is a representative sample. In addition, his data are tied in with those for yet another population for which pursuit data were also taken. Finally, the present pursuit and compensatory display data are compared using both performance measures and the effective open-loop describing function.

Chapter V is devoted to data interpretation. Implications are drawn as to a plausible description of the pilot's utilization of the pursuit display.

Finally, Chapter VI summarizes the general conclusions and findings of the study.

CHAPTER II

SUMMARY OF TRACKING DATA, PURSUIT AND COMPENSATORY DISPLAY COMPARISONS

There have been many studies in which tracking performance for pursuit and compensatory systems has been compared. Initially, perhaps, these were motivated by a desire to demonstrate a clear-cut superiority of one display type over the other. Because the pursuit display provides more information, it was presumed that some advantage would thereby accrue. Indeed, average tracking performance with pursuit systems is often, perhaps even usually, better than that with a compensatory system; but this is by no means the rule. This is attested to by the summary of past pursuit/compensatory comparisons presented in Table I. This is one of our two key starting points. The other, which is a notable omission from the table, is the work of Elkind which will be covered at much greater length as tie-in data for the present series in Chapter IV.

The experiments summarized in Table I can be divided into two categories, corresponding to simple and complex inputs. Only the latter, comprising inputs made up of a minimum of three sinusoids, are of further interest in connection with our data. Of these, the ones of primary interest are the two papers by Chernikoff, et al (Refs. 1, 2), and the comprehensive paper of Obermayer, et al (Ref. 9). Since these consider some of the same controlled elements as examined here, actual comparisons between performance measure data from these sources and those obtained in the present series are given later (Chapter IV).

In a sense the data in this chapter is of limited usefulness, since only performance measures can be compared and as shown in Chapter III this is an insufficient indication of the effects of pursuit versus compensatory displays. In addition, Refs. 1, 2, and 9 used sine waves with harmonic relationships. It is possible that this produced a recognizable pattern which the pilot could utilize to reduce tracking errors below that expected for random appearing inputs.

TABLE I

SUMMARY OF HUMAN OPERATOR TRACKING DATA: PURSUIT AND COMPENSATORY DISPLAY COMPARISONS

AUTHORS	EXPERIMENTAL CONDITIONS					
	Forcing Function	Display	Manipulator	Controlled Element	Performance Measure	Results
Chernikoff, Birmingham, and Taylor (Ref. 1)	Sum of three sinusoids, ω = 0.628, 1.05, 1.57 rad/sec Relative amplitudes, 2.5:1.0:1 Maximum deflection, 4 in.	5 in. CRT, 12 in. from subject, 1/16 in. dia. dot for input or fixed reference, 1/4 in. vertical line for output or error, horizontal displacements	6 in. dia. disk handwheel, 3/4 in. dia. knob at rim, located 10 in. to right of CRT centerline at subject's elbow height	Unaided: $Y_c = K_c$ Aided: $Y_c = K_c\left[1 + \frac{2(0.576)}{0.576}s + \left(\frac{s}{0.576}\right)^2\right]$ $K_c = \frac{0.01 \text{ in. (display)}}{\text{deg (manipulator)}}$	$\int_{15}^{60} \lvert e \rvert \, dt$ for a 1 min. run	Statistical analysis of data for last four sessions of the 10 daily session experiment (6 subjects, 6 trials per condition per day) showed: 1. For the unaided Y_c, pursuit tracking performance was superior to compensatory performance 2. For the aided Y_c, pursuit and compensatory tracking performance were not significantly different 3. For compensatory display, tracking performance with aided Y_c was superior to that with unaided Y_c 4. For pursuit display, tracking performance with aided Y_c was worse than that with unaided Y_c 5. The unaided Y_c pursuit performance was the best of all conditions tested
Chernikoff and Taylor (Ref. 2)	The three-sinusoid frequency content of the three forcing functions was: ω (rad/sec) Slow 0.28, 0.467, 0.70 Med. 0.70, 1.17, 1.75 Fast 1.12, 1.86, 2.79 Relative amplitudes, 2.5:1.5:1 Maximum deflection, 4 in.	5 in. CRT, 12 in. from subject, 1/16 in. dia. dot for input or fixed reference, 1/4 in. vertical line for output or error, horizontal displacements	24 in. long flexible steel bar joystick, located 10 in. to right of CRT centerline and 2 in. above subject's arm rest, deflected laterally, spring gradient of 0.5 lb/in.	Position: $Y_c = K_c$ $K_c = \frac{2 \text{ in. (display)}}{\text{in. (manipulator)}}$ Rate: $Y_c = K_c/s$ $K_c = \frac{4 \text{ in. per sec (display)}}{\text{in. (manipulator)}}$ Aided rate: $Y_c = K_c(1 + 0.5s)/s$ $K_c = \frac{4 \text{ in. per sec (display)}}{\text{in. (manipulator)}}$	$\int_{15}^{60} \lvert e \rvert \, dt$ for a 1 min run	Analysis of data for last four sessions of the 18 daily session experiment (18 subjects, 6 for each forcing function, 3 trials per condition per day) showed: 1. For the medium and fast forcing functions, pursuit tracking performance was superior to compensatory performance for all three Y_c's 2. For the slow forcing function, pursuit tracking performance, compared to compensatory performance, was superior with the position Y_c but was worse with the rate and aided rate Y_c's 3. The best performance was obtained with a compensatory display, aided rate Y_c, and slow forcing function 4. The worst performance was obtained with a compensatory display, rate Y_c, and fast forcing function

TABLE I

(Continued)

AUTHORS	EXPERIMENTAL CONDITIONS					
	Forcing Function	Display	Manipulator	Controlled Element	Performance Measure	Results
Senders and Cruren (Ref. 11)	Sum of two sinusoids, frequencies not specified	CRT, 14 in. from subject's eyes, with a 10-to-the-inch grid, a dot for input or fixed reference, circle for output or error, circle size corresponded to scoring (TOT) area, horizontal displacement	3-1/4 in. fluted knob, rotating in a plane parallel to the display surface, located below and to the right (left for the one left-handed subject) of the CRT center	Position: $Y_c = K_c$ $K_c = \frac{0.0171 \text{ in. (display)}}{\text{deg (manipulator)}}$	Time-on-target (TOT) for a 1 min. run	Analysis of data (5 subjects, 5 trials per condition per day for 5 days) for compensatory, combined (25, 50, and 75 percent pursuit) and pure pursuit displays showed that performance improves significantly when the amount of the pursuit component is increased from zero (compensatory display) to 75 percent, but does not continue to change as the amount of the pursuit component is increased from 75 to 100 percent (pure pursuit).
Poulton (Ref. 10)	Simple harmonic input: Single sinusoids of 1.57, 3.14, 4.71, and 6.28 rad/sec Complex harmonic input: Sum of two sinusoids, lower frequency component same as above, higher frequency component with one-half the amplitude and 1.57 times the frequency	Exposed portions of a mechanical pulley/cable system. For pursuit, input and output were triangular pointers; for compensatory, rhombus pointer moving over a horizontal fixed line. Vertical displacements for both displays.	Wheel with attached horizontal handle, upward movements raising corresponding display pointer	Position: $Y_c = K_c$	$\int_0^{30} \lvert e \rvert \, dt$ for 0.5 min. runs	Relative integrated absolute error data for 32 trials (latin square experimental data with 16 subjects) showed: 1. For all inputs, the pursuit display performance was superior to that for the compensatory display 2. With a pursuit display, the performance was better for the simple input compared to the complex harmonic input 3. With a compensatory display, there was no significant difference in the relative performance for both types of inputs at all speeds
Walston and Warren (Ref. 12)	A single sinusoid of 3.14 rad/sec and a random function with Gaussian amplitude distribution, spectral density peak at 3.14 rad/sec and one-half power points at 1.57 and 4.71 rad/sec Maximum amplitudes, 1/8, 1/4, 1/2, 1, and 2 in.	CRT, 5/8 in. long and 1/32 in. wide vertical line for input or fixed reference, vertical line of same size for output or error, output line below input with slight overlap, horizontal displacements	17 in. lever, low inertia and friction, motion in a horizontal plane with operator resting his elbow on the pivot end of the lever	Position, $Y_c = K_c$ Five K_c's for each input amplitude. For i_{max} = 2 in., K_c = 0.025, 0.05, 0.1, 0.2, and 0.4 in. (display) per deg (manipulator) Gains decreased proportional to decrease in i_{max}	$\frac{1}{60}\int_{15}^{75} e^2 \, dt$ for a 75 sec run Average error, time-on-target, and target hits for several target bands measured but not used	For individual subjects, mean square error performance with the single-sinusoid input is consistently better with the pursuit display than with the compensatory display for all combinations of input amplitude and controlled element gain. This is not true for the random input, although averaged data for four subjects show the pursuit display performance consistently better than that with the compensatory display.

TABLE I

(Continued)

AUTHORS	EXPERIMENTAL CONDITIONS					
	Forcing Function	Display	Manipulator	Controlled Element	Performance Measure	Results
Obermayer, Swartz, and Muckler (Ref. 9)	The three-sinusoid frequency content of the three forcing functions was: ω (rad/sec) Slow 0.14, 0.23, 0.35 Med. 0.28, 0.47, 0.70 Fast 0.70, 1.16, 1.75 Relative amplitudes, 2.5 1.5:1 Average absolute and root mean square magnitude: μ (in.) $\overline{\lvert i \rvert}$ (in.) Slow 0.94 0.81 Med. 0.92 0.77 Fast 0.88 0.74	5 in. CRT, 28 in. from subject, 2 in. long horizontal line for input or fixed reference, inverted "T" with 1 in. long horizontal line and 0.5 in. vertical line for output or error, vertical displacements	22 in. long center-positioned joystick, deflected fore and aft, maximum deflections ±6 in. at top, breakout force of 0.5 lb, spring gradient of 1 lb/in., ±1/8 in. deadband in circuitry	Position: $Y_c = K_c$ $K_c = \frac{0.5 \text{ in. (display)}}{\text{in. (manipulator)}}$ Rate: $Y_c = K_c/s$ $K_c = \frac{1 \text{ in. per sec (display)}}{\text{in. (manipulator)}}$ Acceleration: $Y_c = K_c/s^2$ $K_c = \frac{4 \text{ in. per sec}^2 \text{ (display)}}{\text{in. (manipulator)}}$	$\frac{1}{T}\int_0^T e\,dt$, $\frac{1}{T}\int_0^T \lvert e \rvert\,dt$, $\frac{1}{T}\int_0^T e^2\,dt$, time-on-target (TOT) with tolerance band of ±1/10 in., and hits (number of times $\lvert e \rvert < 1/10$ in.), T = 60.43 sec	Average data for six subjects, 10 trials per condition showed: 1. There is no statistically significant difference between pursuit and compensatory displays for three cases: the slow input with position control and the medium input with rate and acceleration control 2. The pursuit display performance was significantly worse than that with the compensatory display for three cases: the slow input with rate and acceleration control and the fast input with acceleration control 3. The pursuit display performance was significantly better than that with the compensatory display for three cases: the medium input with position control and the fast input with position and rate control 4. The rank order of average absolute and mean square error scores is the same, and the significant differences occur for both performance measures 5. The best performance occurred with the slow input, compensatory display and rate control; the worst performance with the fast input, pursuit display and acceleration control 6. For all display and controlled element combinations, performance deteriorated with increased forcing function speed 7. For all forcing function display combinations except the slow input with compensatory display, performance deteriorated with increased controlled element order

TABLE I

(Concluded)

AUTHORS	EXPERIMENTAL CONDITIONS					
	Forcing Function	Display	Manipulator	Controlled Element	Performance Measure	Notes
Hartman (Refs. 4, 5)	Single sinusoids, frequencies 1.05, 2.09, 3.14, 4.19, 5.23, and 6.28 rad/sec Maximum deflection, 7 in.	21 in. CRT, 101 in. from subject, 5/8 in. long and 1/16 in. wide vertical line for input or fixed reference, vertical line of same size for output or error, input line just above horizontal midline of scope, output mounted below, horizontal displacements	12-1/2 in. springless joystick free to move in two dimensions, side-to-side movements for control, maximum deflection ±3-3/4 in.	Position: $Y_c = K_c$ $K_c = \frac{2 \text{ in. (display)}}{\text{in. (manipulator)}}$	Time-on-target (TOT) and number of hits for last 75 sec of 105 sec tracking run, scoring and +0.7 in.	[illegible] ght subjects, three runs per [illegible], showed: [illegible] the pursuit display [illegible] with the compensatory [illegible] [illegible] display, there was no sign[illegible] change in TOT performance with input [illegible]y 3. With the pursuit display, rather large differences in input frequency were necessary to produce a significant difference in TOT scores; performance data iorating with increased frequency

CHAPTER III

BLOCK DIAGRAM STRUCTURE, PURSUIT DETECTION TECHNIQUES AND EXPERIMENTAL CONFIGURATION

The first purpose of this chapter is to discuss the system relationships that can result from the pilot's utilization of the information in the pursuit display. Possible block diagram organizations are presented and their implications for the experimental detection of pursuit organization, as well as its measurement, are examined. Awkward measurement problems arise because pursuit behavior implies two or more pilot describing functions operating with a single forcing function. The explicit determination of the pilot's describing functions requires two or more independent inputs — unfortunately, the addition of a second input increases the number of task variables and therefore modifies the control task. Finally, the chapter concludes with a discussion of the experimental configuration.

A. BLOCK DIAGRAM STRUCTURE

With a pursuit display the operator sees both the input, i, and output, m, of the system, and has as his task the minimization of their difference, the system error, e. The possible block diagram structure representing the operator's response in this situation is shown in Fig. 3, where Y_{p_i}, Y_{p_e}, and Y_{p_m} are describing functions indicating the operations on i(t), ϵ(t), and m(t), respectively. An integral part of the quasi-linear system description is the remnant, $n_c(t)$, injected at the pilot's output to account for the portion of the response that is not linearly correlated with the system input, i(t).

The presence of a pursuit display does not guarantee that the pilot will utilize all the information presented. Table II summarizes the six possibilities.

Using Fourier transforms, the equations of motion are

$$C = IY_{p_i} + EY_{p_e} + MY_{p_m} + N_c \qquad (1)$$

$$E = I - M \qquad (2)$$

$$M = CY_c \qquad (3)$$

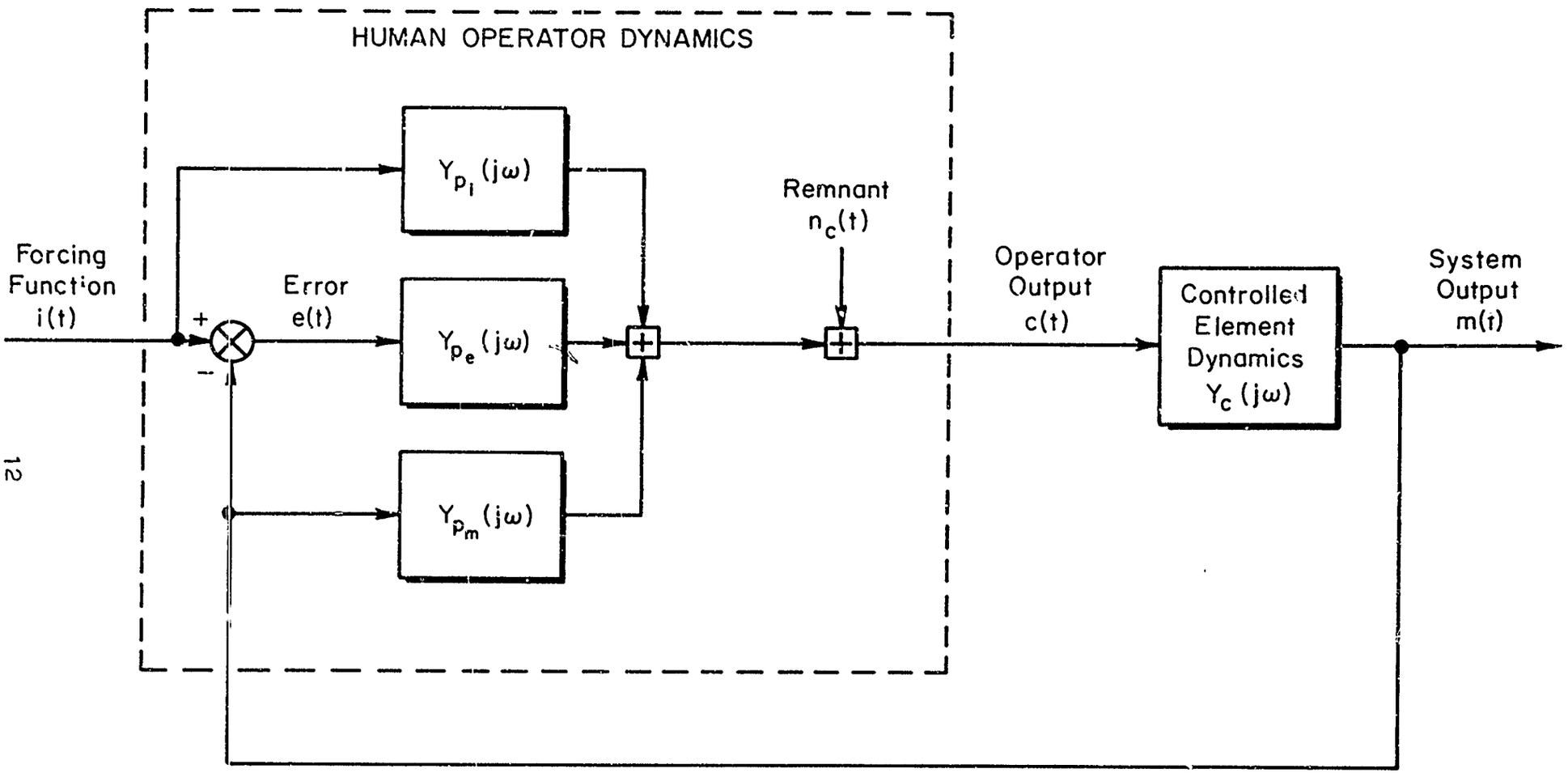

Figure 3. General Block Diagram of the Human Operator in a Pursuit Display Tracking Task

TABLE II

POSSIBLE HUMAN OPERATOR RESPONSE STRUCTURES FOR PURSUIT DISPLAYS

TITLE	SYSTEM PARAMETERS USED*
Compensatory.....	e
Compensatory and feedforward.....	e , i
Compensatory and inner loop.....	e , m
Compensatory, inner loop, and feedforward.	e , m , i
Inner loop and feedforward.....	m , i
Pure feedforward.....	i

*For a pursuit display only two parameters are independent since e - m.

Solving for the pilot's output and system error and system output yields

$$C = \underbrace{\left[\frac{Y_{p_i} + Y_{p_e}}{1 + Y_c\left(Y_{p_e} - Y_{p_m}\right)}\right]}_{\frac{\Phi_{ic}}{\Phi_{ii}}} I + \underbrace{\left[\frac{1}{1 + Y_c\left(Y_{p_e} - Y_{p_m}\right)}\right]}_{\frac{\Phi_{n_c c}}{\Phi_{n_c n_c}}} N_c \qquad (4)$$

$$E = \underbrace{\left[\frac{1 - Y_c\left(Y_{p_m} + Y_{p_i}\right)}{1 + Y_c\left(Y_{p_e} - Y_{p_m}\right)}\right]}_{\frac{\Phi_{ie}}{\Phi_{ii}}} I - \underbrace{\left[\frac{Y_c}{1 + Y_c\left(Y_{p_e} - Y_{p_m}\right)}\right]}_{\frac{\Phi_{n_c e}}{\Phi_{n_c n_c}}} N_c \qquad (5)$$

$$M = \underbrace{\left[\frac{Y_c\left(Y_{p_i} + Y_{p_e}\right)}{1 + Y_c\left(Y_{p_e} - Y_{p_m}\right)}\right]}_{\frac{\Phi_{im}}{\Phi_{ii}}} I + \underbrace{\left[\frac{Y_c}{1 + Y_c\left(Y_{p_e} - Y_{p_m}\right)}\right]}_{\frac{\Phi_{n_c m}}{\Phi_{n_c n_c}}} N_c \qquad (6)$$

In Eqs. 4–6 the parts of E, C, and M which are correlated with the input are noted by the ratios of the cross-spectra with respect to I.

Since i and n_c are uncorrelated, the error spectral density is given by

$$\Phi_{ee} = \left|\frac{1 - Y_c\left(Y_{p_m} + Y_{p_i}\right)}{1 + Y_c\left(Y_{p_e} - Y_{p_m}\right)}\right|^2 \Phi_{ii} + \left|\frac{Y_c}{1 + Y_c\left(Y_{p_e} - Y_{p_m}\right)}\right|^2 \Phi_{n_c n_c} \qquad (7)$$

and the mean-squared error by

$$\overline{e^2} = \frac{1}{2\pi}\int_0^\infty \Phi_{ee}(\omega)\, d\omega = \overline{e_i^2} + \overline{e_n^2} \qquad (8)$$

where

$$\overline{e_i^2} = \frac{1}{2\pi}\int_0^\infty \left|\frac{1 - Y_c\left(Y_{p_m} + Y_{p_i}\right)}{1 + Y_c\left(Y_{p_e} - Y_{p_m}\right)}\right|^2 \Phi_{ii}\, d\omega \qquad (9)$$

and

$$\overline{e_n^2} = \frac{1}{2\pi}\int_0^\infty \left|\frac{Y_c}{1 + Y_c\left(Y_{p_e} - Y_{p_m}\right)}\right|^2 \Phi_{n_c n_c}\, d\omega \qquad (10)$$

The ratio

$$Y_\beta = \frac{\Phi_{im}}{\Phi_{ie}} = \frac{Y_c\left(Y_{p_i} + Y_{p_e}\right)}{1 - Y_c\left(Y_{p_m} + Y_{p_i}\right)} \qquad (11)$$

has the property that the portions of M and E linearly correlated with the input are described by

$$\frac{M}{I} = \frac{Y_\beta}{1 + Y_\beta} \qquad (12)$$

$$\frac{E}{I} = \frac{1}{1 + Y_\beta} \qquad (13)$$

independent of the type of display or pilot utilization. Thus Y_β is the effective open-loop describing function, and has essentially the same interpretation in the pursuit as in the compensatory situation. That is, a single loop closure about Y_β results in the closed-loop characteristics.

To reduce tracking errors at low frequency the pilot should adjust his describing function boxes such that $Y_\beta \gg 1$ at $\omega < \omega_c$. For the compensatory display this has to be accomplished by a single describing function Y_{p_c} operating on the error, whereas Y_{p_m}, Y_{p_i}, and Y_{p_e} are theoretically available in pursuit.

In terms of Y_β the characteristic equation is given by

$$1 + Y_\beta = 0 \tag{14}$$

or

$$\frac{1 + Y_c\left(Y_{p_e} - Y_{p_m}\right)}{1 - Y_c\left(Y_{p_m} + Y_{p_i}\right)} = 0 \tag{15}$$

Setting the numerator of Eq. 15 to zero gives the same characteristic equation as implied by the denominators in Eqs. 4–6.

Using Eq. 13, the mean-squared error correlated with the forcing function, $\overline{e_i^2}$, is related to Y_β as

$$\overline{e_i^2} = \frac{1}{2\pi}\int_0^\infty \left|\frac{1}{1 + Y_\beta}\right|^2 \Phi_{ii}\, d\omega \tag{16}$$

An example of a simple change in Y_β is an increase in the effective crossover frequency, and if $Y_\beta \doteq \omega_{c_\beta} e^{-j\omega\tau}/j\omega$, then in a fashion analogous to the compensatory situation (Ref. 7),

$$\frac{\overline{e_i^2}}{\sigma_i^2} \doteq \frac{1}{3}\left(\frac{\omega_i^2}{\omega_{c_\beta}^2}\right) \quad \text{if} \quad \omega_i \ll \omega_{c_\beta} \tag{17}$$

where the effective crossover frequency is defined by $\left|Y_\beta(j\omega_{c_\beta})\right| = 1$.

B. DETECTION OF PURSUIT BEHAVIOR

For the same input and controlled element, the detection of differences between compensatory and pursuit behavior has, in the past, relied primarily on performance measures. A key feature of the experimental program reported here is that comparisons were also made in terms of the effective open-loop

describing function, Y_β, which reveals the dynamic effects of the pilot's system organization. The inadequacy of $\overline{e^2}$ alone is revealed by Eq. 8, i.e., a change in $\overline{e^2}$ could be due to a change in either $\overline{e_i^2}$ or $\overline{e_n^2}$. It is also possible that the change from a compensatory to a pursuit display would produce no change in $\overline{e^2}$ but equal and opposite changes in $\overline{e_i^2}$ and $\overline{e_n^2}$. From these factors it is seen that the detection of pursuit/compensatory differences requires the comparison of two quantities, such as $\overline{e^2}$ and Y_β, or both $\overline{e^2}$ and $\overline{e_i^2}$ (where the latter reflects Y_β).

As opposed to <u>detection</u> there are two major unknowns which contribute to the problem of <u>directly measuring</u> human operator describing function characteristics for pursuit display tracking These are:

1. The actual block diagram structure adopted by the operator, i.e., the system parameters used to generate his output, is not known, nor is there any knowledge that the same block diagram structure exists for all inputs and controlled elements. Note that of the three unknown boxes in Fig. 3 only two are independent.

2. A second input that is statistically independent of the primary input (forcing function) is required to obtain data for computing the describing functions of the two elements. It is desired that the control situation be characterized only by the forcing function i(t) and the controlled element. Therefore the second input must be such that it does not influence the operator's normal pursuit response characteristics to the forcing function, and at the same time must be of sufficient amplitude to permit accurate cross-spectral or equivalent measurements.

The requirement that the second input be uncorrelated with the forcing function further compounds the problem of directly computing both operator describing function elements. Without loss of generality, we can assume that $Y_{p_m} = 0$. If the second input, d(t), is injected downstream of the pilot's output, c(t), the cross-spectra ratios are

$$\frac{\Phi_{ic}}{\Phi_{ie}} = \frac{Y_{p_i} + Y_{p_e}}{1 - Y_c Y_{p_i}} \qquad (1$$

$$\frac{\Phi_{dc}}{\Phi_{de}} = Y_{p_e} \qquad (19)$$

Thus Y_{p_e} is measured directly by the second input and Y_{p_i} can be calculated from Eq. 18. Note that for inputs which are sums of sine waves the cross-spectra ratios exist only at the sine wave frequencies of each input. Thus for i(t) and d(t) to be independent there can be no common frequencies; therefore Eqs. 18 and 19 cannot be solved directly. Two procedures could be used in an attempt to resolve this difficulty.

1. Interpolate the Φ_{ic}/Φ_{ie} and Φ_{dc}/Φ_{de} data to the d and i frequencies, respectively.
2. Interchange some of the forcing function and second input frequencies, thus obtaining Φ_{ic}/Φ_{ie} and Φ_{dc}/Φ_{de} data at the same frequencies but from separate runs.

The problems discussed above apply to the direct measurement of the operator's describing function characteristics for pursuit tracking, and are applicable to the general multiloop measurement task. An alternate procedure for obtaining additional insight into the human operator's pursuit describing functions is to perform the experiments without the second input and apply the analysis technique discussed in Chapter V.

C. EXPERIMENTAL SITUATION

The experimental arrangement and measurement techniques are nearly identical to those in Ref. 7. Thus, the following sections will briefly discuss the situation for this experimental series only as it differs from that of Ref. 7.

1. Physical Layout and Equipment

The experiments were performed in a laboratory area consisting of two connected rooms. The larger of the two rooms contained all of the electronic equipment for performing and analyzing the experiments. The smaller room contained the manipulator and display. In this way the operator is isolated from the measuring equipment and other disturbances. The describing function data were obtained using the watthour-meter analyzer described in Ref. 7. This machine evaluates the real and imaginary parts of the Fourier coefficient of the e, c, and m signals using each input frequency as a reference. In addition, each run was recorded on magnetic tape.

The general measurements and task variables involved in the experiments are shown in Fig. 4. The task variables used in this experimental series are shown in dashed boxes, i.e., the forcing function and the controlled element. The Y_c's used were

$$K_c$$

$$K_c/s$$

$$K_c/s^2$$

$$\frac{K_c}{s(s-\lambda)} \qquad \lambda = 0.5,\ 1.0,\ 1.5$$

$$\frac{K_c(s+0.25)}{(s+5)^2}$$

These controlled elements were selected to provide a very broad coverage of pilot equalization to close the loop, ranging over very low frequency lags to essentially pure gain to low frequency leads (Ref. 7).

2. Forcing Function

The forcing functions, i(t), used in the pursuit experiments were of the augmented rectangular input spectrum form but with two different frequency spacings. One set was identical to that in Ref. 7 and spectra using this frequency spacing are designated by ω_i, σ_i, where ω_i is the cutoff frequency in radians/second and σ_i is the rms amplitude in inches, i.e., as seen on the display. The other set is designated by either B5, σ_i, or R14, σ_i, a notation similar to that in Ref. 3. The following paragraph describes the frequency content and bandwidth of the various inputs. The rms values used are discussed in Chapter IV and indicated in Table III.

The frequency setting, ω_n, and the number of periods, n_r, for each component in the fixed 240-sec run length, T_R, are given on p. 20. For the ω_i, σ_i spacings three approximate ω_i values were used — 1.5, 2.5 and 4.0 rad/sec. To define these three inputs, the amplitudes at the lowest

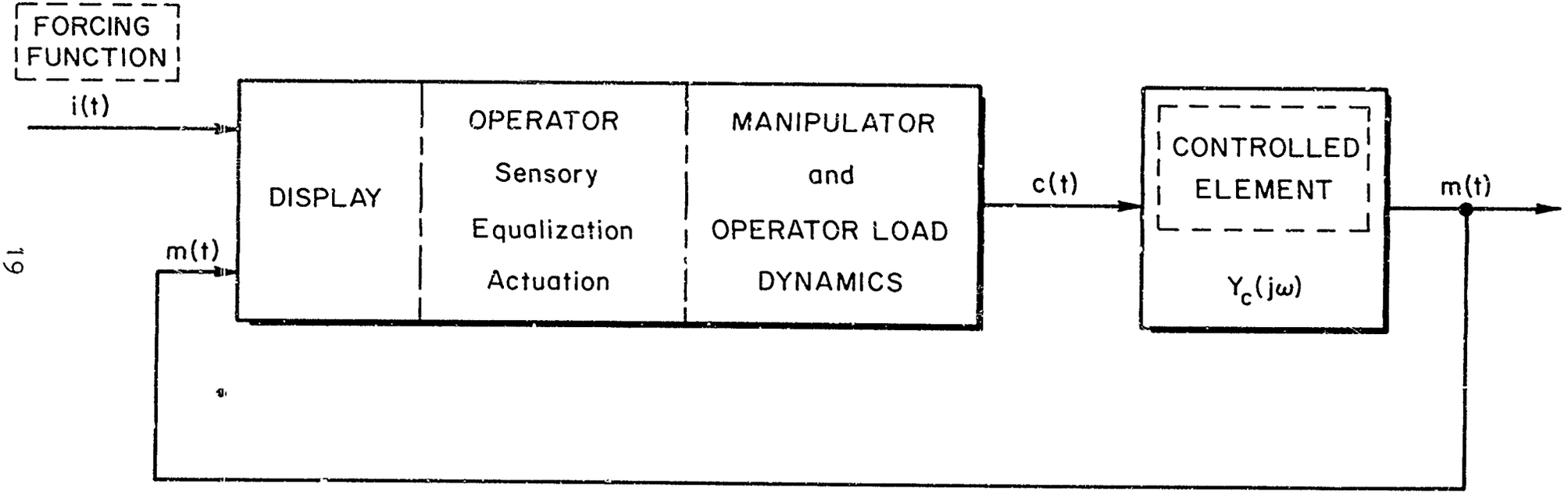

Figure 4. General Measurements and Task Variables

six, seven, or eight frequencies were set equal, for cutoff frequencies of 1.49, 2.54, or 4.03 rad/sec, respectively. The amplitudes of the remaining frequencies were set to one-tenth of the low frequency amplitudes (20 db attenuation). The logarithmic spacing (which facilitates fitting ratios of rational polynomials to the measured values) was selected to insure the effective independence of the sine wave components over the run length of interest.

ω_i, σ_i		B5, σ_i; R14, σ_i	
ω_n	$n_r = T_R\omega_n/2\pi$	ω_n	$n_r = T_R\omega_n/2\pi$
0.157	6	0.314	12
0.262	10	0.732	28
0.393	15	1.151	44
0.602	23	1.675	64
0.969	37	1.989	76
1.49	57	2.407	92
2.54	97	4.29	164
4.03	154	6.17	236
7.57	289	10.14	388
13.8	527	14.03	536

For the other forcing functions all the amplitudes were equal for the R14, σ_i input, while the four highest frequencies were attenuated 10 db for the B5, σ_i input. Figure 5a shows measured input power spectral magnitudes for the three ω_i forcing functions, while Fig. 5b provides a similar picture for the B5 and the R14 spectra.

The forcing functions selected serve several purposes. The range of forcing functions is covered by the augmented ω_i spectra; these are also appropriate for direct tie-in and extension of the Ref. 7 results. These would be sufficient except that, in the major past study (Ref. 3), two interesting pursuit/compensatory differences were found for high bandwidth forcing function spectra. These were:

- Above a particular forcing function bandwidth, compensatory rms error becomes less than the pursuit rms error.

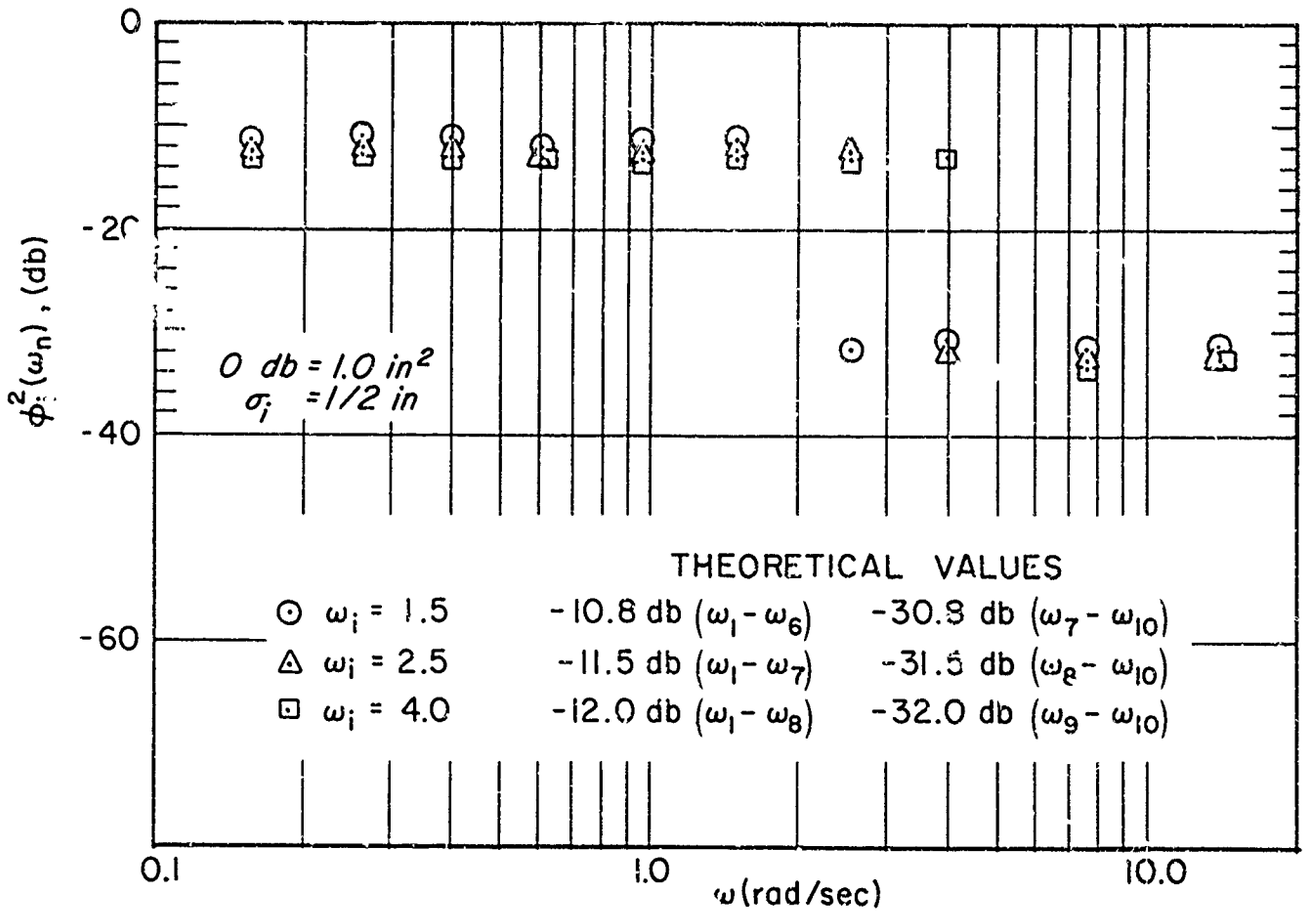

a) ω_i = 1.5, 2.5, 4.0

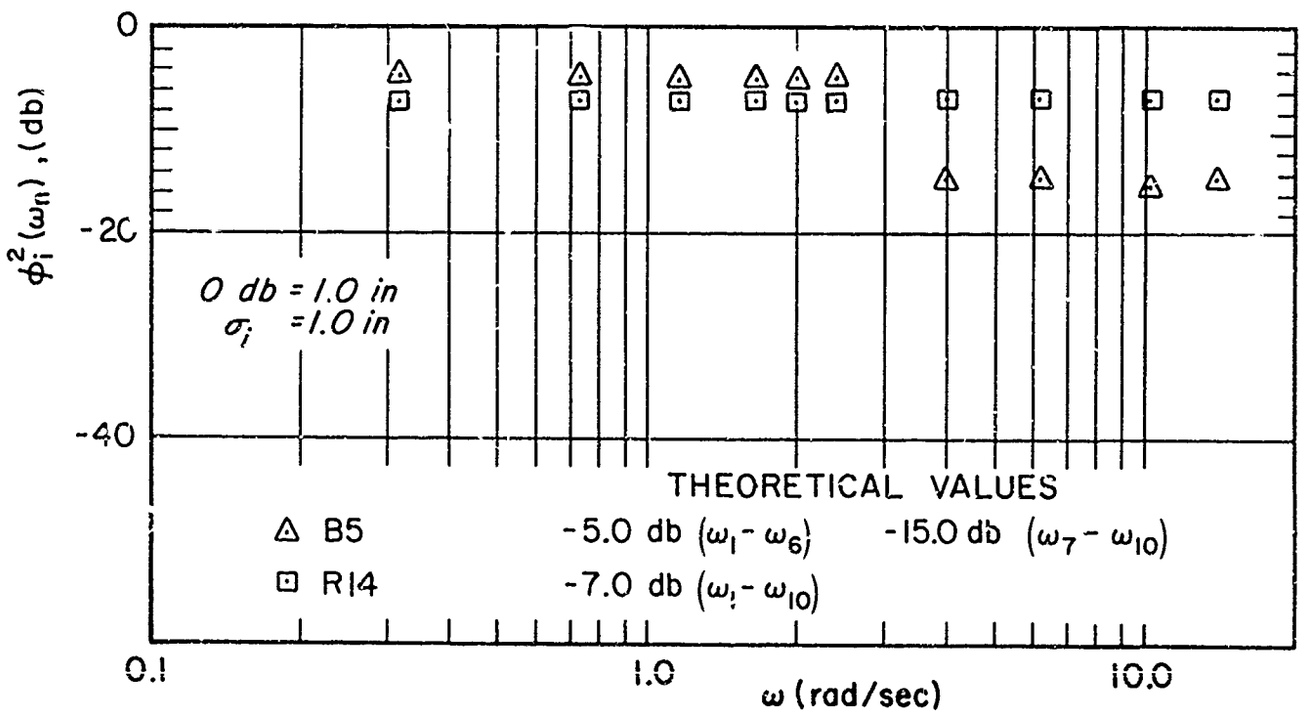

b) B5, R14

Figure 5. Measured Forcing Function Power Spectra Magnitude

- At a still higher forcing function bandwidth, a pursuit system is still operable, but compensatory cannot be controlled by the operator.

The high frequency bandwidth(s) serve to further explore these conditions.

3. Display and Manipulator Sensitivities

The pursuit display is shown in Fig. 6, where the dot for the input and the vertical line for the system output move laterally. The pilot's output, c(t), consisted of lateral motions of a spring-restrained side stick (negligible inertia and damping). For a pure gain controlled element of unity, the display and stick are related by

K_S = 1 in. (display)/6° (stick)

F_S = 2.21 oz/deg (stick) (applied at top of 4-in. stick)

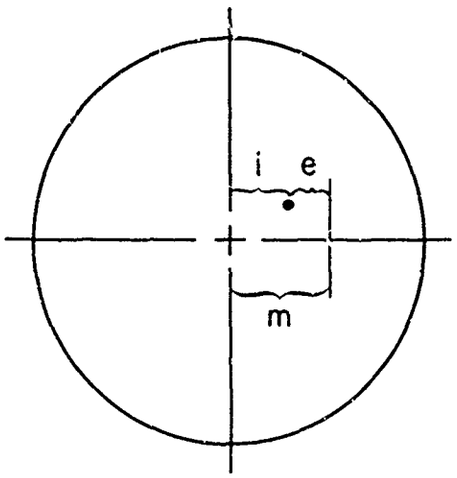

Figure 6. Pursuit Display

With the 4-in. moment arm, lateral motion of the operator's hand amounts to about 0.07 in. (stick) per degree of stick rotation. Accordingly, the sensitivity can be expressed in terms of the linear motion of the operator's hand by dividing the angular sensitivity (in inches per radian) by the moment arm, i.e.,

$$K_S = 1 \text{ in.}/6^\circ \times 57.3^\circ/\text{rad} \times 0.25 \text{ in.}^{-1}$$
$$= 2.38 \text{ in. (display)/in. (stick)}$$

For controlled elements other than unity, all of the above sensitivities are multiplied by $Y_c(j\omega)$ and they become dynamic quantities.

The pilot/manipulator/display configuration is depicted in Fig. 7. Only the roll axis was used for this experimental series. Movements of the stick in one direction produced system output movements in the same direction.

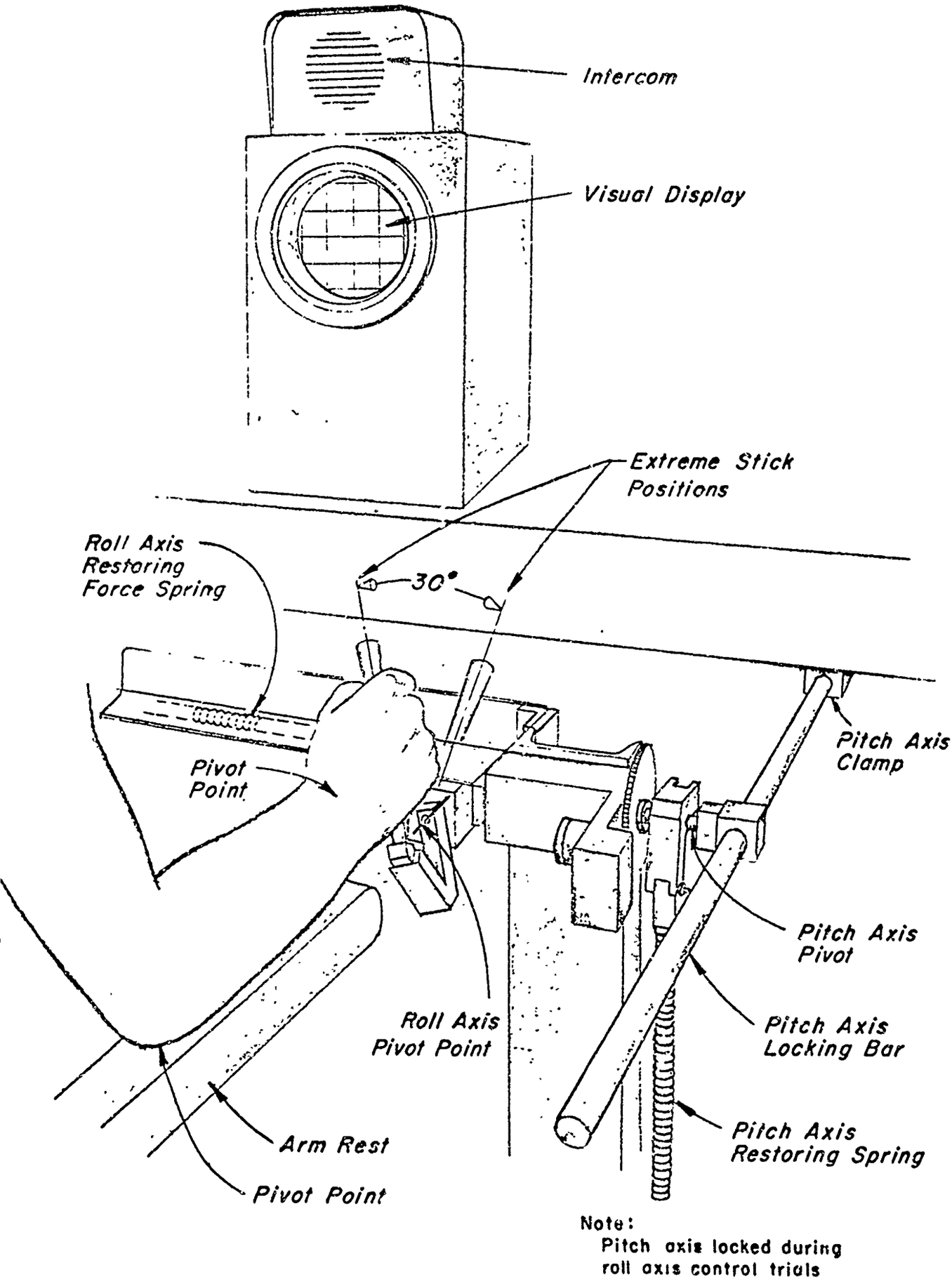

Figure 7. Stick Manipulator

CHAPTER IV

EXPERIMENTAL DATA

This chapter presents the experimental describing function and performance measure data. For this sort of exploratory study a design which includes a large number of forcing functions and controlled elements is essential. This would be excessively expensive if several subjects were used. Consequently, in the interests of economy and maximum coverage a single well-trained subject was used throughout with several special restrictions to increase the likely generality of the results. These were:

- Tie-in of this set of experiments with those involving a large population of pilots to indicate that the subject used was a representative sample (Ref. 7).
- Tie-in of this set with the only previous comprehensive describing function measurements (Ref. 3), thereby corroborating those findings and indicating a reasonable tie-in to yet another population.

The particular controlled elements, forcing functions, and display configurations tested are shown in Table III. Exceptions to the rms input values are indicated by an asterisk. The numbers in each cell indicate the run sequence. Each configuration was repeated three times using a single highly motivated subject who was a light-airplane-qualified civilian pilot with extensive tracking experience. Because of his experience the subject was able to rapidly approach asymptotic values of performance on any given configuration, thereby permitting a large number of configurations to be examined at minimal cost. While more subjects would have been desirable, the exploratory and limited-effort nature of the experimental series made this unrealistic. To make the results as representative as possible, considerable effort was made to tie them in to other data.

In what follows Section A presents the subject's compensatory display data to tie in with that in Ref. 7 for a population of pilots and that in Ref. 3 (where pursuit data were also taken). Also included is a comparison

TABLE III

RUN SEQUENCE (THREE REPLICATIONS PER CONFIGURATION)

CONTROLLED ELEMENT Y_c	FORCING FUNCTION										σ_i (in.)
	Compensatory Display					Pursuit Display					
	1.5	2.5	4.0	B5	R14	1.5	2.5	4.0	B5	R14	
K_c	13	15	17	1	3	14	16	18	2	4	1.0
$\frac{K_c}{s}$	19	21	23	5	7	20	22	24	6	8	1/2
$\frac{K_c}{s^2}$	25	27	29	9	11*	26	28	30	10	12*	1/2 *σ_i = 1/4
$\frac{K_c}{s(s - 0.5)}$	31					32					1/4
$\frac{K_c}{s(s - 1.0)}$	33					34					1/4
$\frac{K_c}{s(s - 1.5)}$	35					36					1/4
$\frac{K_c(s + 0.25)}{(s + 5.0)^2}$	37	39	41			38	40	42			1.0

of long term effects for the present subject to demonstrate the typical asymptotic performance levels achieved by human operators. These tie-ins and long term effects increase the generality of the pursuit/compensatory comparisons in later sections. Section B compares the performance measure results with those of other experiments. Section C presents a detailed comparison of Pursuit and Compensatory performance measures obtained in this study. Finally, Section D compares the describing functions for compensatory and pursuit display.

A. COMPENSATORY DATA COMPARISONS

1. Population of Pilots (Ref. 7)

In general the describing function data, Figs. 8–11, indicate that the present subject is typical of a pilot population. Note that the data from Ref. 7 (circles) are plotted at the correct input frequencies, whereas the current data have been shifted slightly to the right to avoid overlapping. In each case the data points indicate mean values; the vertical lines indicate $\pm 1\sigma$ spread. For easy controlled elements (K_c and K_c/s) and for low bandwidth inputs, there is no difference between the present subject and the other pilots (Ref. 7). For the harder controlled elements and higher bandwidth inputs, the present subject usually has a higher crossover frequency and low frequency gain, plus less effective time delay near crossover and above. These differences are probably due to the extensive tracking experience of the present subject (close to 500 data runs plus numerous practice runs) compared to the eight other pilots used in the Ref. 7 series.

To illustrate the long term effects of practice, consider Figs. 12 and 13 for $Y_c = K_c$ and $K_c/s(s-1.5)$, respectively. Figure 12, for the relatively easy but extremely well-practiced case of $Y_c = K_c$, shows amazingly close agreement for test periods over one year apart. Even the subtler data trends are closely duplicated in this comparison, and we conclude that the subject's describing function had stabilized. (The slight improvement in tracking error is probably due to reduced remnant.) Figure 13 shows a similar comparison for the second-order unstable element in which $\lambda = 1.5$ (near the uncontrollable limit). Even in this much more difficult case the agreement is quite good, except that there is less tracking error and high frequency phase lag, indicating a refined tracking technique over the intervening year.

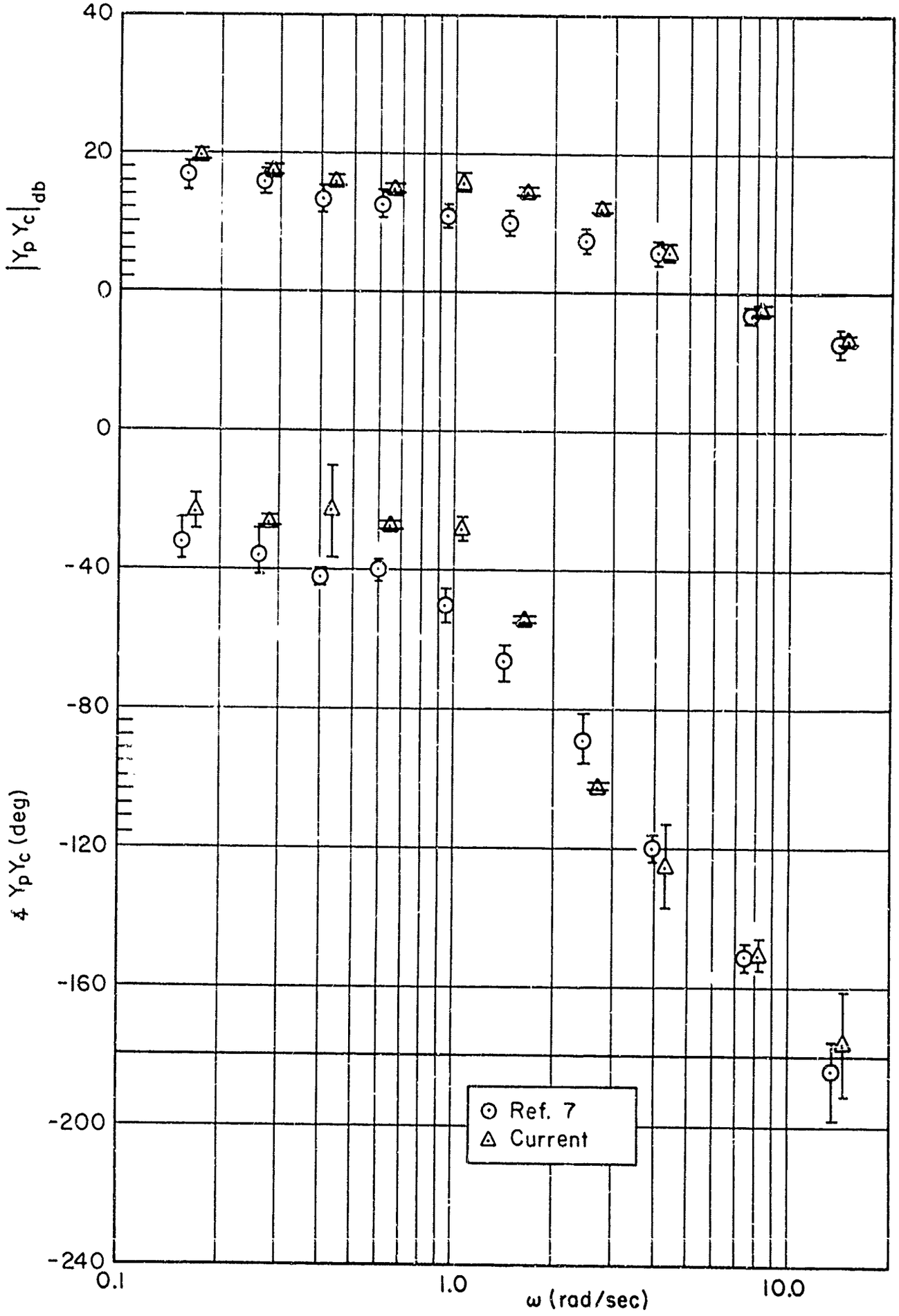

Figure 8. Comparison of Compensatory Display Data with Population of Pilots; $Y_c = K_c$, $\omega_1 = 2.5$

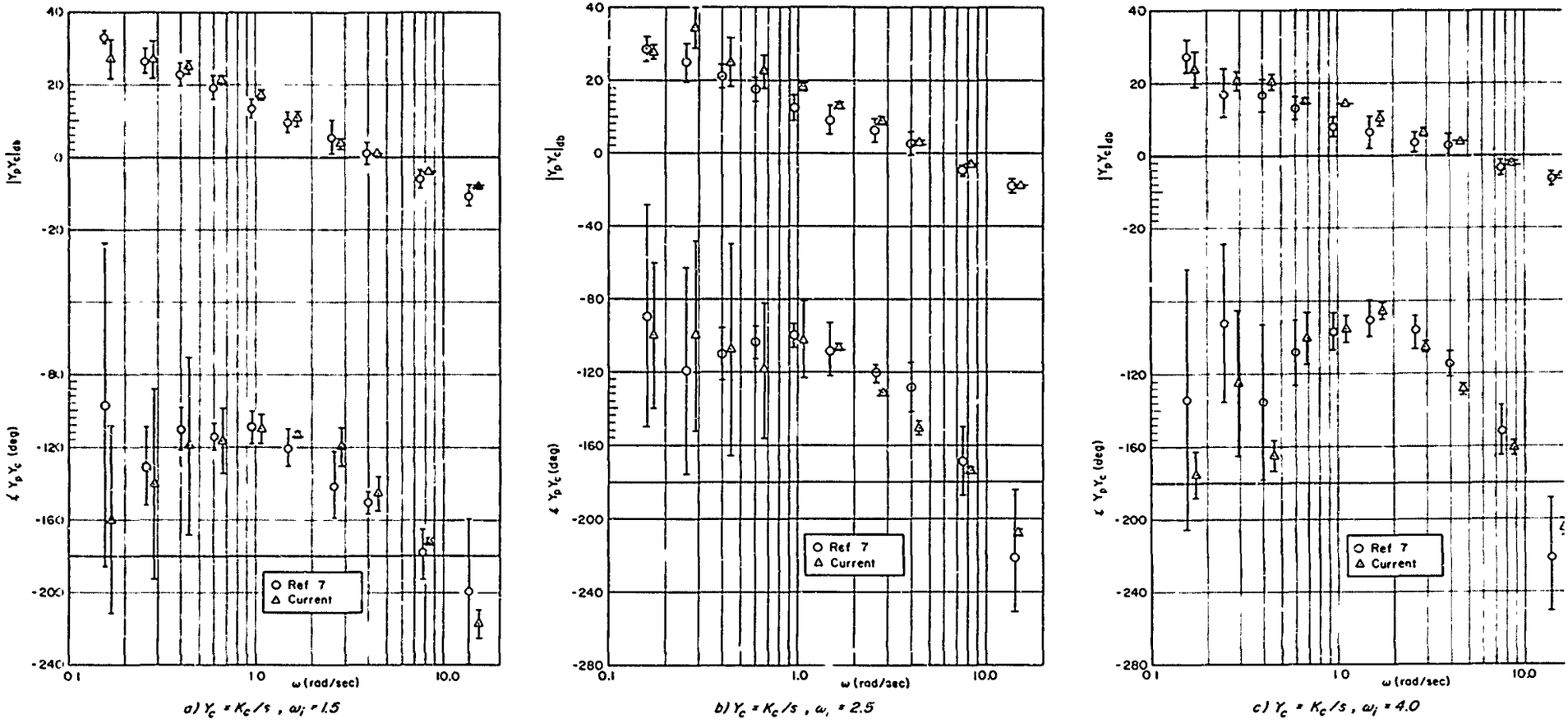

Figure 9. Comparison of Compensatory Display Data with Population of Pilots

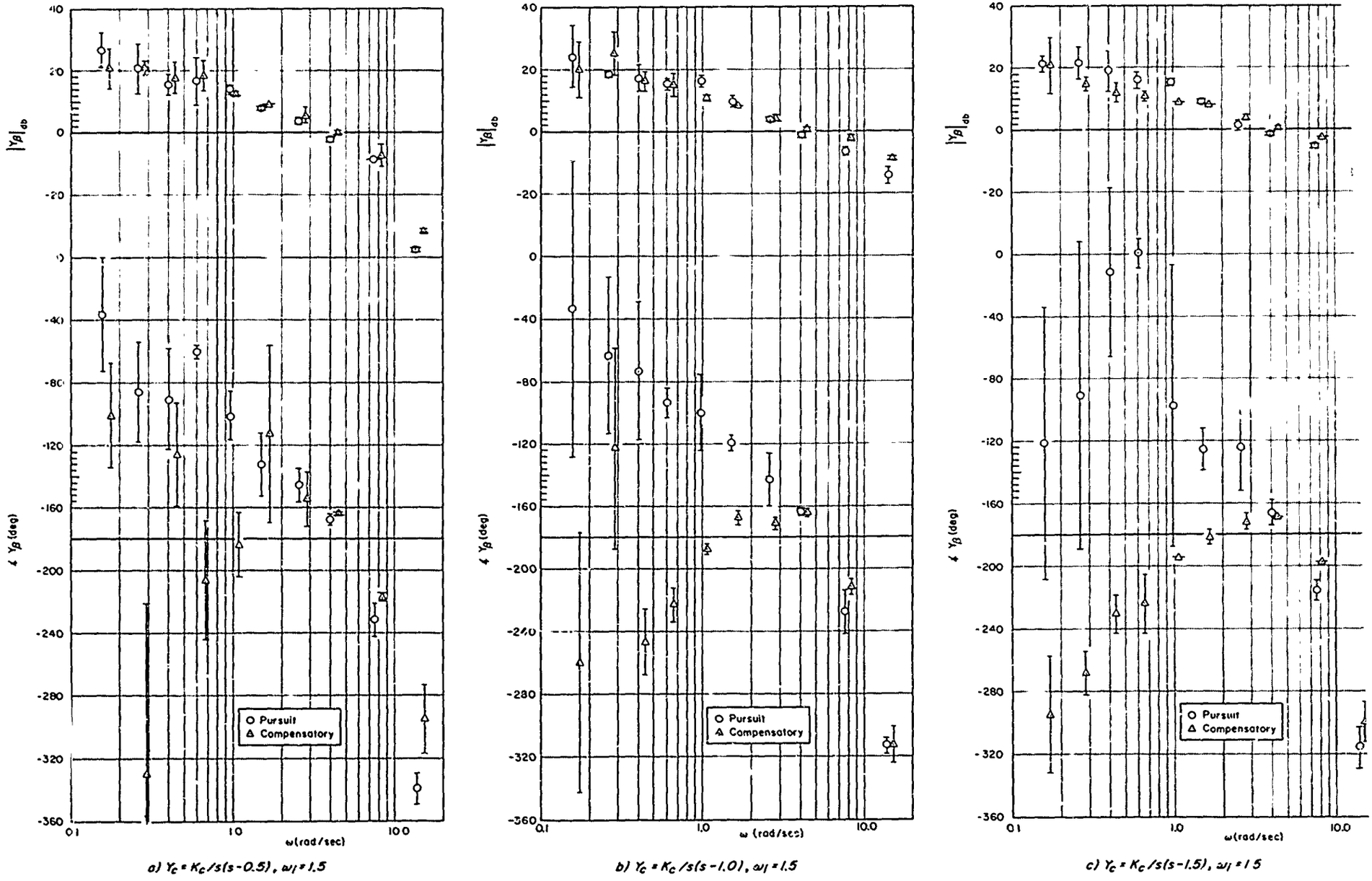

Figure 10. Comparison of Compensatory Display Data with Population of Pilots

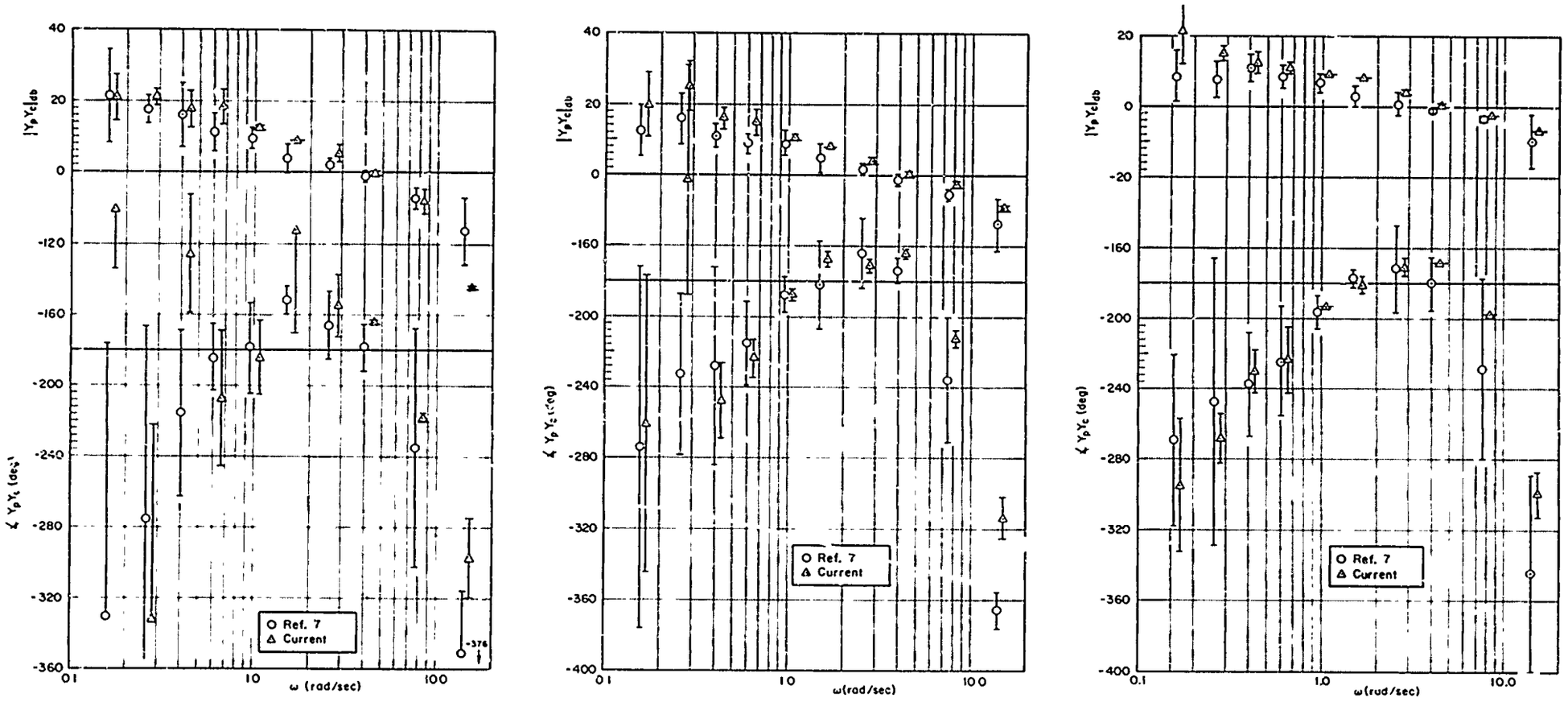

Figure 11. Comparison of Compensatory Display Data with Population of Pilots

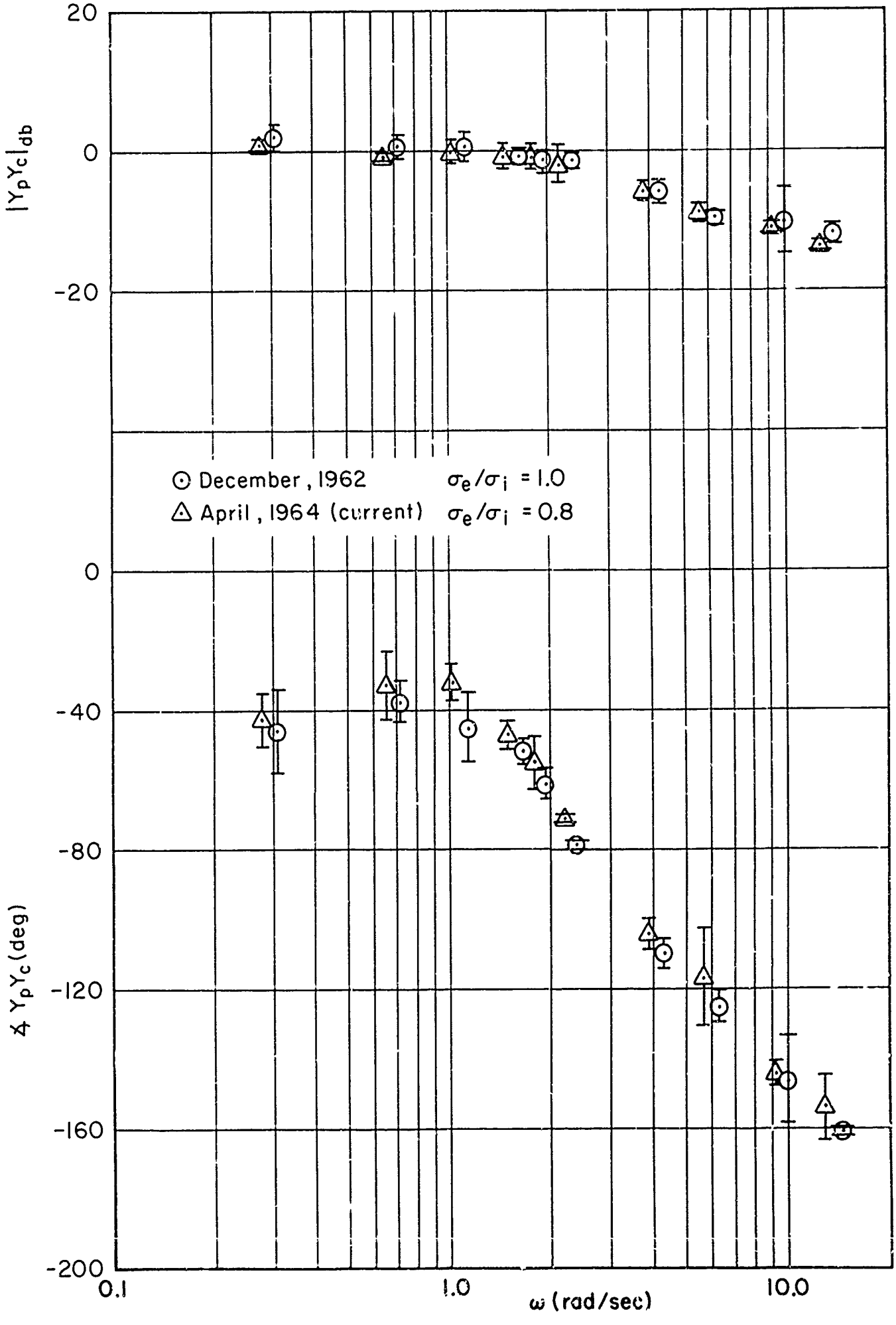

Figure 12. Long Term Variability of the Current Subject's Describing Function $Y_c = K_c$, R14 Input

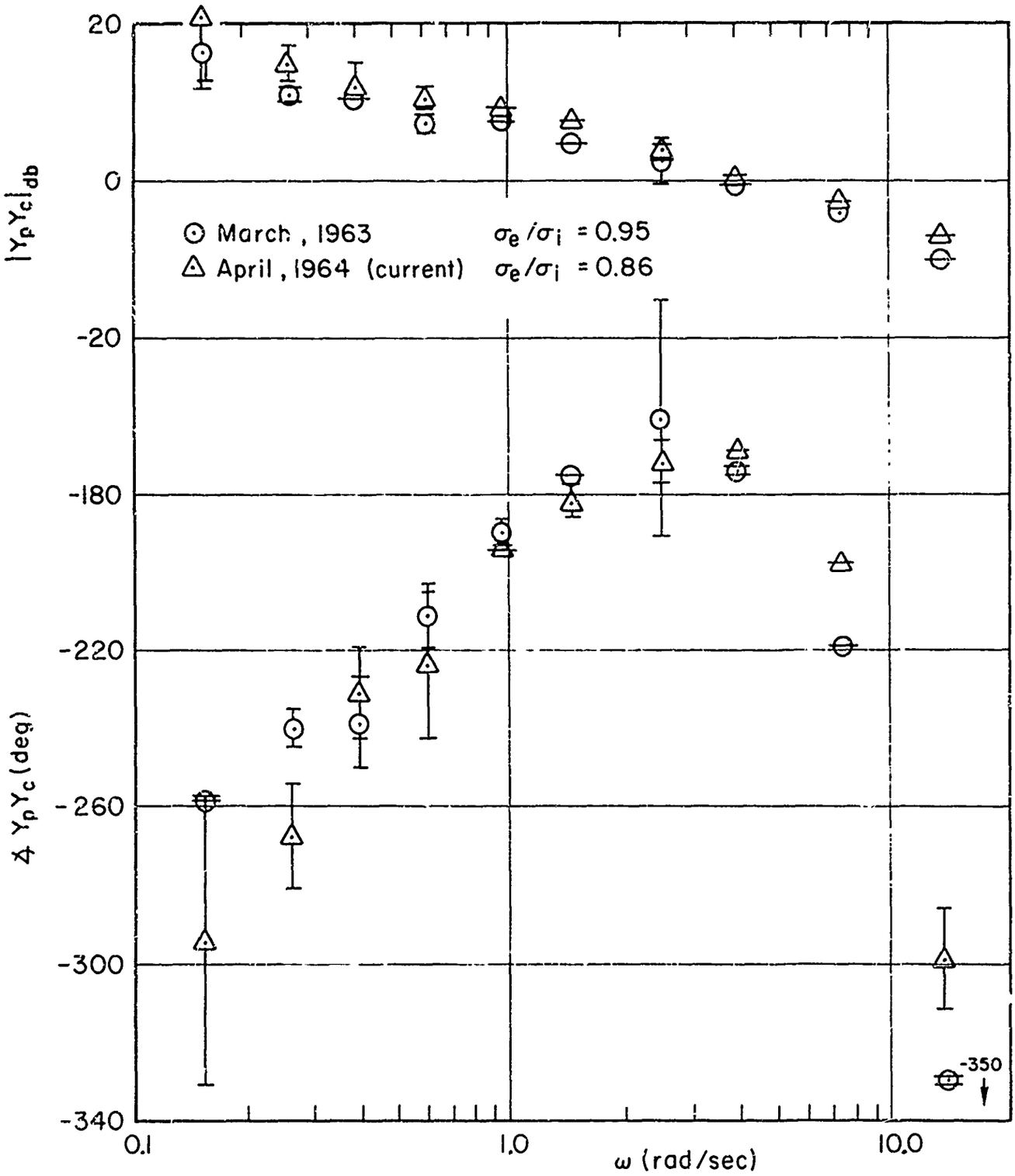

Figure 13. Long Term Variability of the Current Subject's Describing Function $Y_c = K_c/s(s-1.5)$, $\omega_c = 1.5$

While skill level differences may explain some of the differences between the present subject and the population of pilots, it's quite likely that our subject's extensive tracking experience is the largest factor. Thus, our single subject can be considered typical of a pilot population in that they will reach an asymptotic level of performance in their well-trained flying tasks in analogous fashion to the present subject in tracking tasks.

2. Population of Students (Ref. 3)

In order to tie in with the body of data generated from $Y_c = K_c = 1$ in Ref. 3, a tracking situation as similar as possible to Elkind's had to be considered in both Ref. 7 and the present experiments. Ideally, the tie-in experiments should be conducted with forcing functions and manipulators similar to those to be used in our other experiments, yet also similar enough to Elkind's to effect a reasonable connection. Fortunately, Elkind's B6 forcing function amounts, in our notation, to $\omega_1 = 3.0$, 1 in., so the $\omega_1 = 2.5$, 1 in., forcing function was thought to provide reasonably close approximation. The lightly restrained stick manipulator used in this series and Ref. 7 differs substantially in form from Elkind's freely moving pencil-like pip tracker, although the movements in both cases were generally lateral (with more rotation involved in Ref. 7 and the present series). Yet, in our past work we were able to show reasonable connections with Elkind's data even using an aircraft center stick (Ref. 8), so any differences due to the manipulators were expected to be slight.

In Ref. 7 three highly trained pilots tracked two runs each for $Y_c = K_c = 1$, 2, and 5, respectively. The differences between Y_p measurements for successive runs for each pilot were very slight; the two runs were averaged and are shown in Y_pY_c form in Fig. 14 along with the corresponding compensatory display data from the current experiments. Elkind's comparable data for $\omega_1 = 3.0$, 1 in., are also shown in Fig. 14. These data are averages of four four-minute runs, two from one subject and one run from each of two other subjects. It is clear from Fig. 14 that the results are remarkably compatible with the Elkind data, with the current subject giving a slightly better match for low frequency

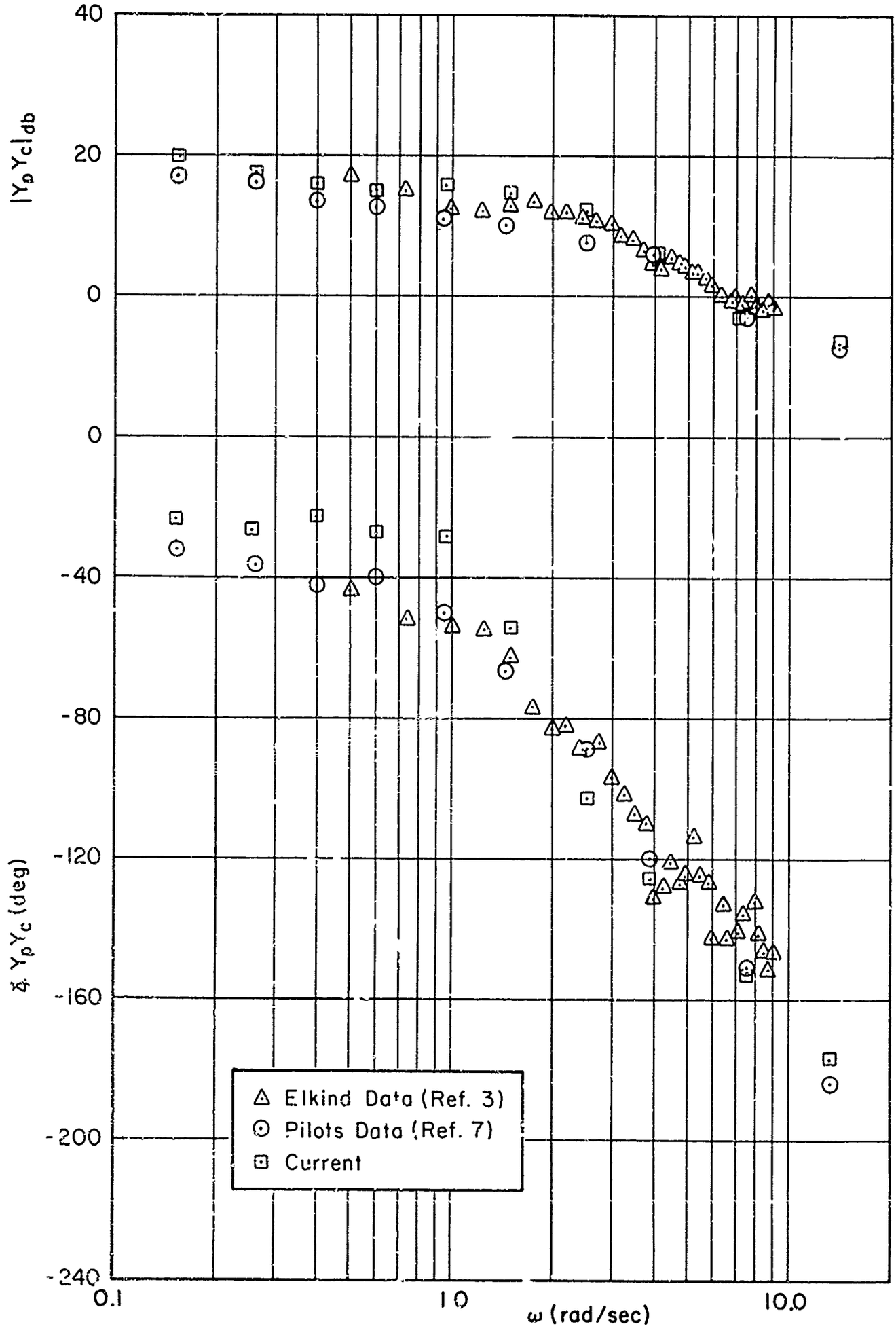

Figure 14. Comparison of Current $_{1_C} = K_C$ Data with Elkind's Data

amplitudes. In fact, this extremely close correspondence between data taken years apart, by different experimenters at different locations, with different subjects, different analysis apparatus, and slightly different forcing functions and manipulators, etc., is very satisfying especially considering the subject selection procedures:

- Reference 7 used three naval test pilots, each trained to a stable performance level (as measured by $\overline{e^2}/\sigma_i^2$) for each configuration.
- The current series used a single subject with extensive tracking experience.
- Reference 3, utilized highly trained students.

Thus, all indications are that the current single subject has reached a stable performance level against which to compare his pursuit display data in Subsections B, C, and D below, increasing the generality of the conclusions drawn there.

B. COMPARISON OF PERFORMANCE MEASURES WITH RESULTS OF OTHER EXPERIMENTERS

While our describing function data can only be compared with Elkind's, the performance measure results can be compared with those of Refs. 1, 2, 3, 9. Figure 15 shows the normalized mean-squared error for pursuit and compensatory obtained in our series with those found by Elkind. Our augmented rectangular forcing function spectra are similar to his rectangular spectra, differing primarily by the addition of a few low amplitude waves to form a high frequency shelf. Thus, the Elkind R.24, R.4, and R.64 forcing function spectra (where the .24, .4, and .64 are in cycles/second) correspond roughly to our ω_1 = 1.5, 2.5, and 4.0 rad/sec, respectively. Also, our R14 (highest frequency, 14 rad/sec) spectrum is akin to his R1.6 or R2.4. As indicated in Fig. 15, the trends between compensatory and pursuit exhibited by the two sets of data are generally similar; both sets of data indicate lower mean-squared error for the pursuit display except at the higher forcing function bandwidths (B5, R14, and R2.4). Although Elkind had a forcing function similar to B5, the relative mean-squared errors for this input are not available.

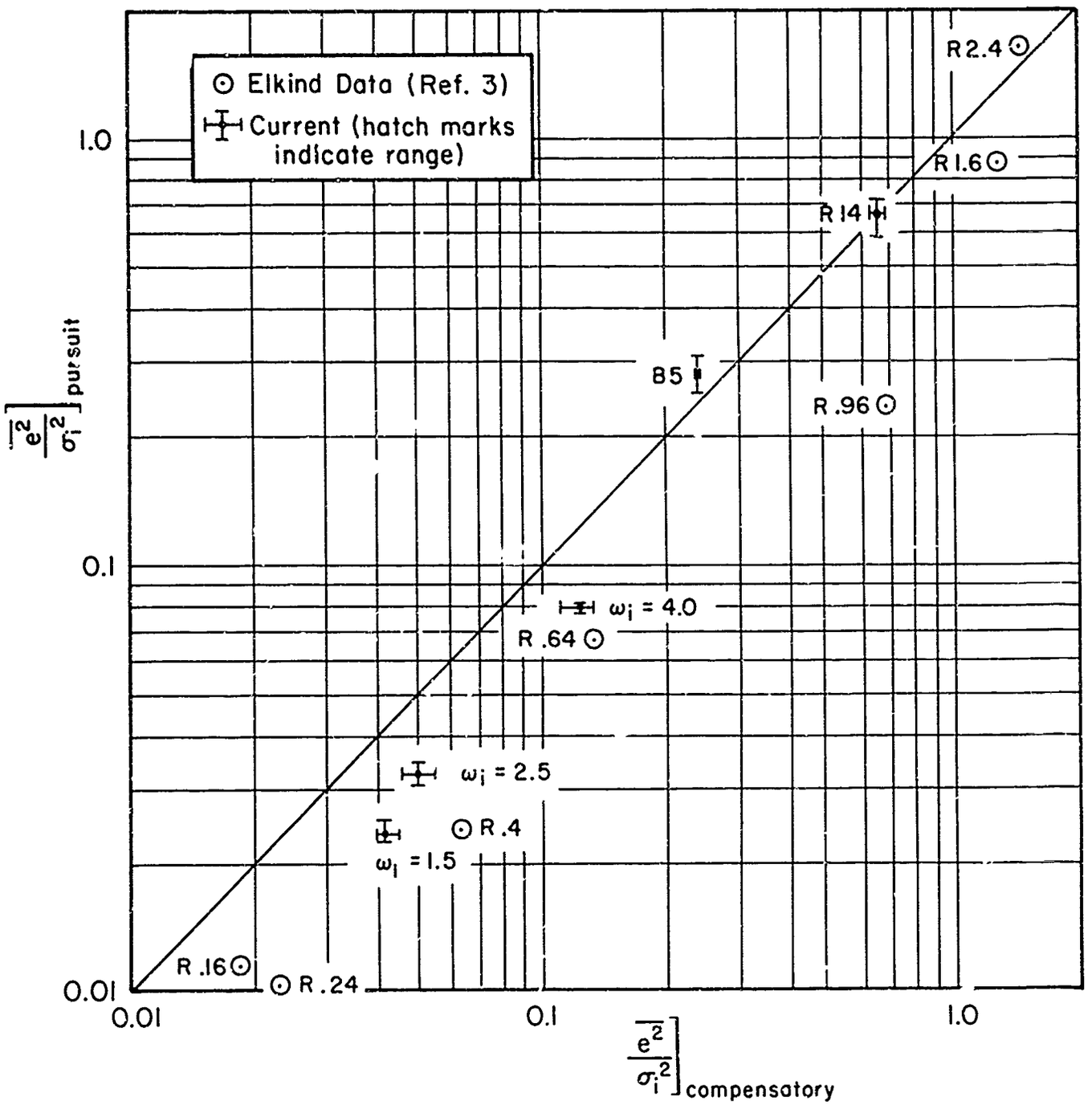

Figure 15. Performance Measure Comparisons with Elkind's Results, $Y_c = K_c$

Another comparison for $Y_c = K_c$ is made on the basis of the data from Refs. 1 and 9. In both these experimental series only three sinusoids were used to make up the forcing function. These input spectra do not have a meaningful "bandwidth" as such. Consequently, to show a rough comparison between these and our results they are classified in terms of the maximum forcing function frequency (neglecting the high frequency shelf in our data). The result for $Y_c = K_c$ is shown in Fig. 16. The indications are that all the data are reasonably comparable, and that pursuit performance measures are smaller than compensatory for all but the very lowest frequency input used in Ref. 9.

Similar comparisons for $Y_c = K_c/s$ and K_c/s^2 are also shown in Fig. 16. These comparisons are both ambiguous and confusing. For $Y_c = K_c/s^2$, for example, the current data and those of Ref. 2 indicate that pursuit is superior, whereas the data of Ref. 9 show precisely the opposite. For $Y_c = K_c/s$ both Ref. 2 and Ref. 9 are in opposition to our results for higher frequency forcing functions, although they both also indicate compensatory is better than pursuit at lower frequencies, a trend that would coincide with our results. Finally, the lowest frequency forcing function for Ref. 2 is in direct opposition for the medium frequency input of Ref. 9. The causes of such differences are subtle indeed, for critical examination of the conflicting data shows no defect in method or procedures. About the only conclusion that can be drawn from the $Y_c = K_c/s$ data is that performance with either form of display can be superior to the other under highly restricted circumstances.

C. COMPARISON OF PURSUIT AND COMPENSATORY PERFORMANCE MEASURES

Figures 17 - 21 present the performance measures obtained with pursuit data plotted on the ordinates and compensatory data on the abscissas. Both the total relative mean-squared error, $\overline{e^2}/\sigma_i^2$, and its components ($\overline{e_i^2}/\sigma_i^2$, $\overline{e_n^2}/\sigma_i^2$) are presented. These figures also contain plots of $\overline{c^2}$, $\overline{c_i^2}$, and $\overline{c_n^2}$ (not normalized). The average performance measures are given at the intersections of the lines which have short hatch marks on their ends to indicate the range of the measurements.

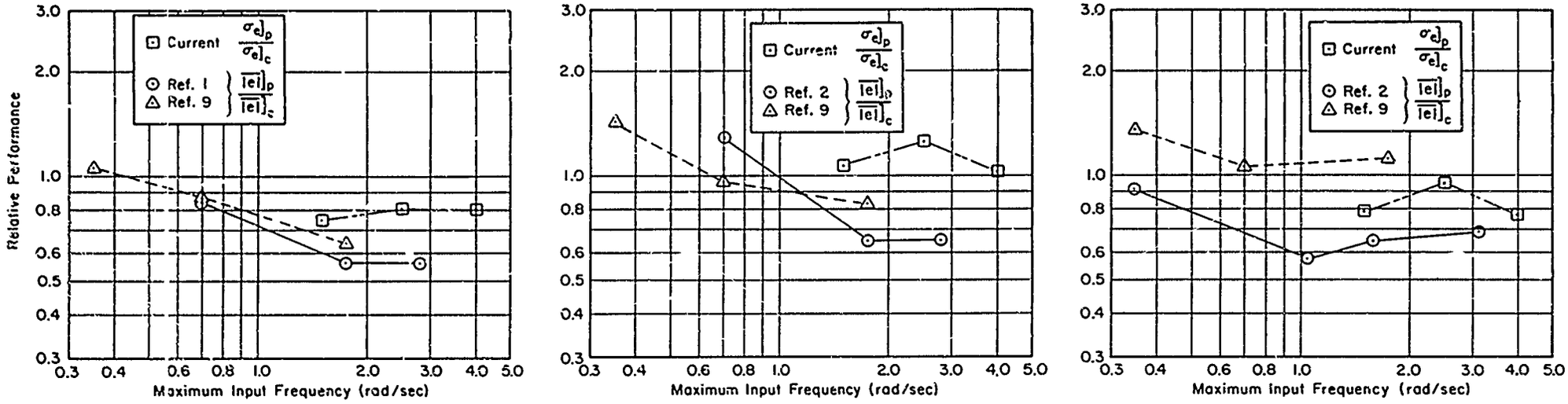

a) $Y_c = K_c$

b) $Y_c = \frac{K_c}{s}$

c) $Y_c = \frac{K_c}{s^2}$

$Y_c = \frac{K_c}{s(s + 0.15)}$ (Ref. 2)

Figure 16. Relative Performance Measure Comparisons with Refs. 1, 2, and 9

$Y_c = K_c$, K_c/s, and K_c/s^2

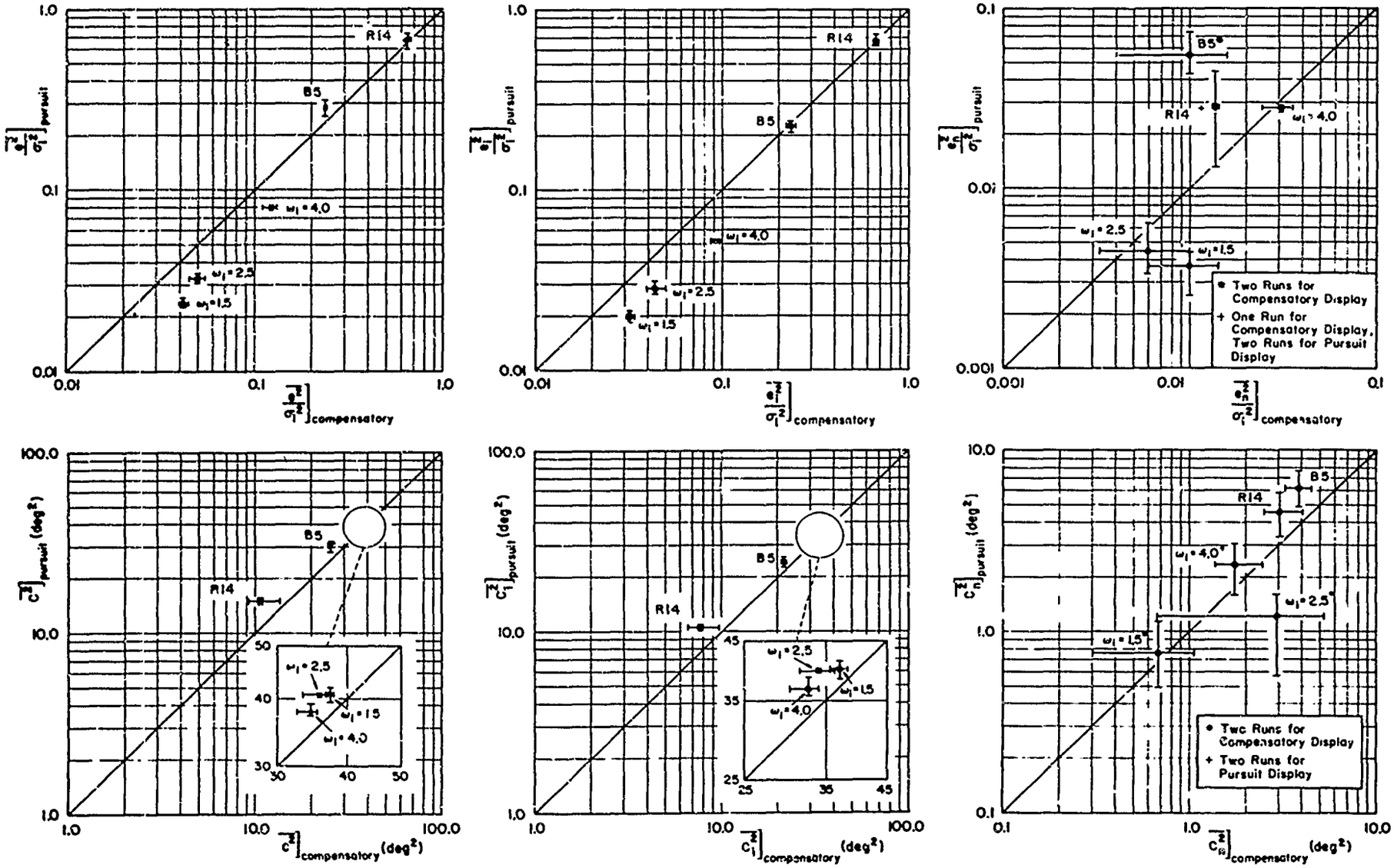

Figure 17. Performance and Control Deflection Data; $Y_c = K_c$

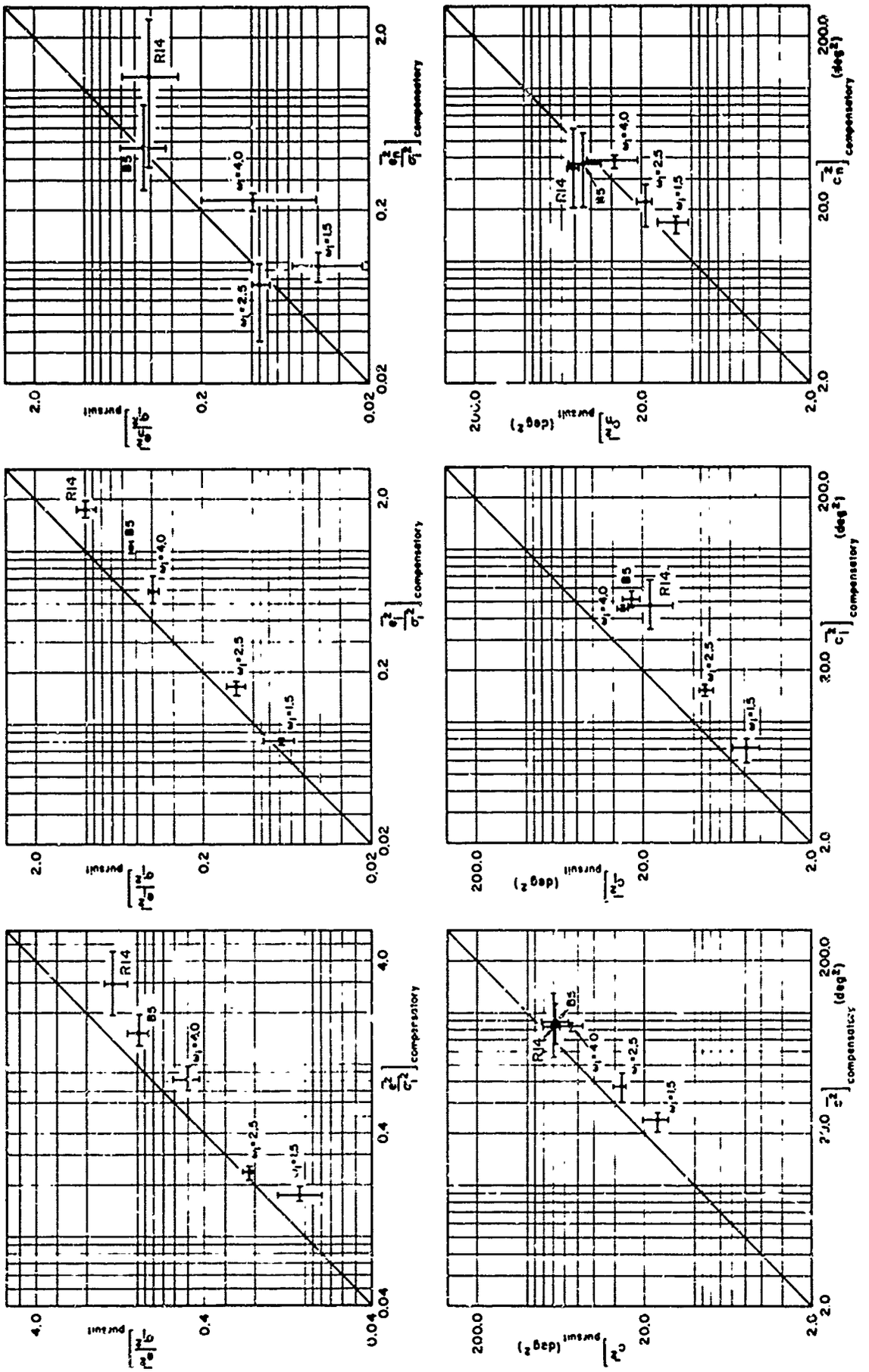

Figure 18. Performance and Control Deflection Data; $Y_c = K_c/s^2$

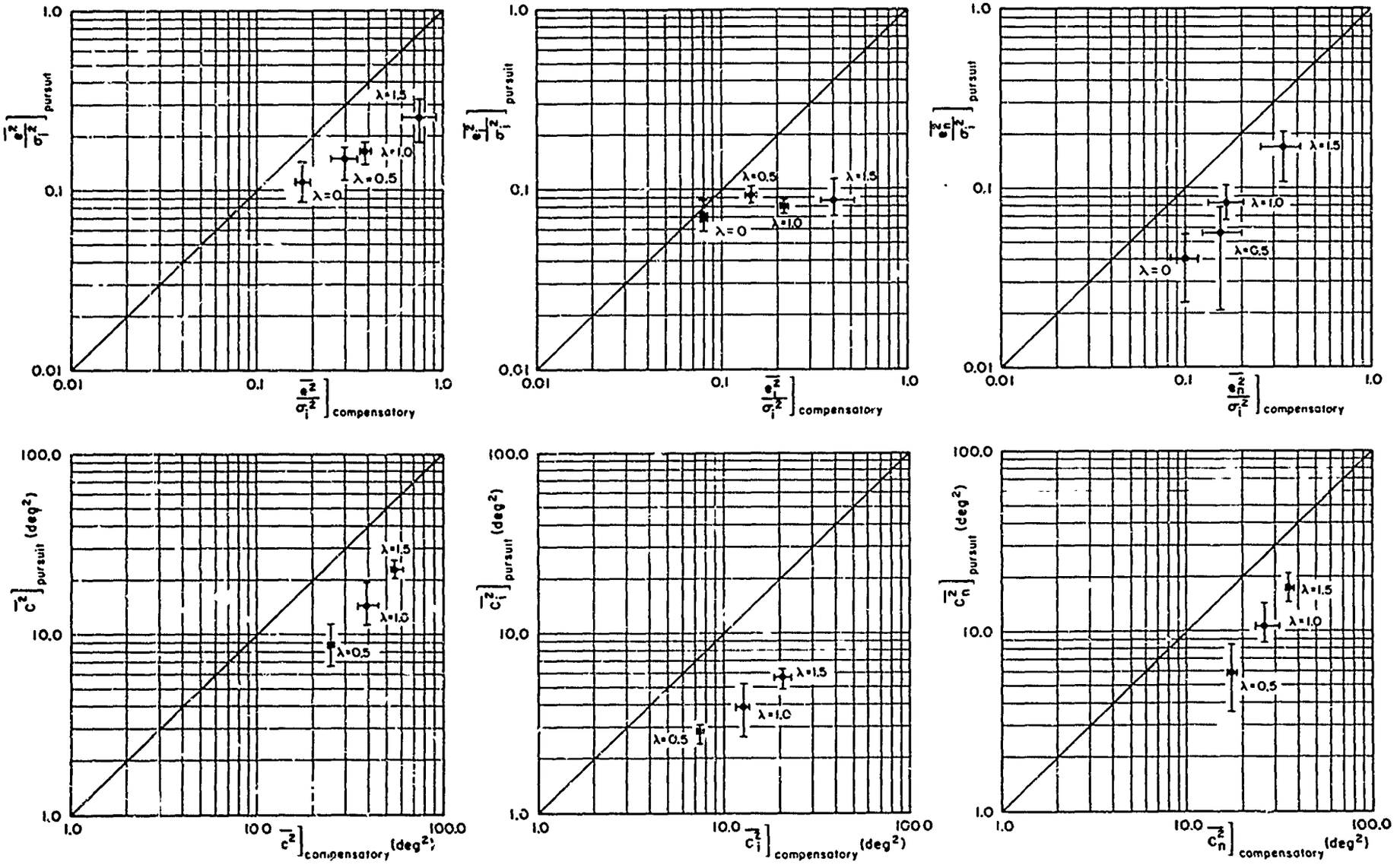

Figure 19. Performance and Control Deflection Data; $Y_c = K_c/s(s - \lambda)$

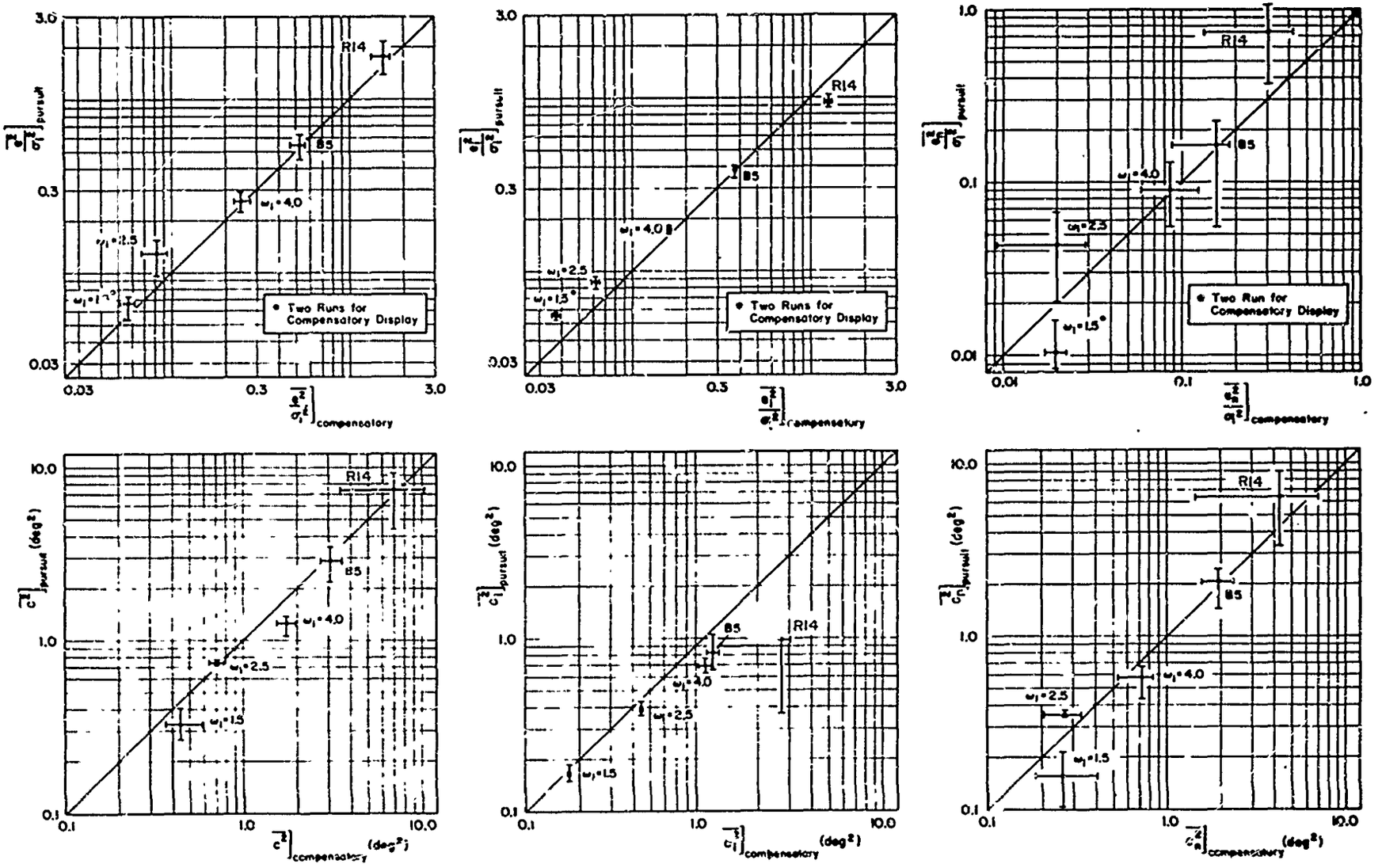

Figure 20. Performance and Control Deflection Data; $Y_c = K_c/s$

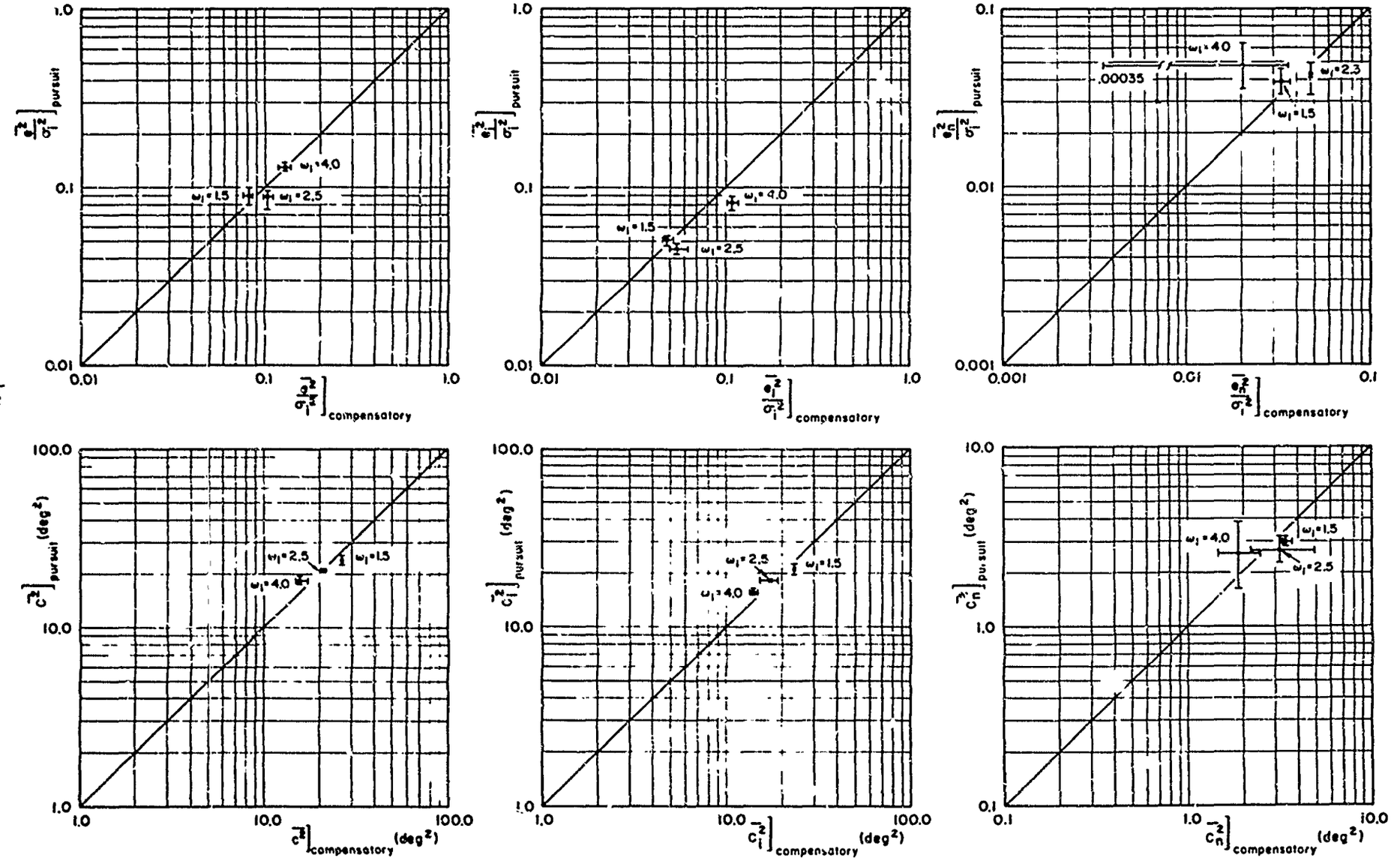

Figure 21. Performance and Control Deflection Data; $Y_c = K_c(s+0.25)/(s+5)^2$

A summary of the performance measures ($\overline{e^2}$, $\overline{e_i^2}$, and $\overline{e_n^2}$) is given in Table IV, where the letters "P" (pursuit) or "C" (compensatory) indicate the configuration having the smaller measure. In Figs. 17–21 when the equivalent (i.e., P = C) line falls within the range of measures a "PC" or "CP" is used, with the first symbol indicating the smaller mean. The numbers in parentheses are the relative rms performance measures. The results for the five configurations have been grouped into those showing clear superiority of the pursuit display [$Y_c = K_c$, K_c/s^2, and $K_c/s(s-\lambda)$], e.g., the relative rms performance measure is about 0.8, and those showing little or no consistent difference [$Y_c = K_c/s$ and $K_c(s+0.25)/(s+5)^2$]. More detailed conclusions are for:

$Y_c = K_c$ (Fig. 17)

Pursuit is better than compensatory for both $\overline{e^2}$ and $\overline{e_i^2}$ for low bandwidth inputs (augmented ω_i spectra), becoming essentially the same for high bandwidth inputs (B5 and R14) (This was discussed in Subsection B above.) Note that while $\overline{e_n^2}$ is erratic it is quite small, so that it has little effect on $\overline{e^2}$.

$Y_c = K_c/s^2$ (Fig. 18)

Generally pursuit is increasingly better than compensatory as ω_i increases for both $\overline{e^2}$ and $\overline{e_i^2}$. Results for $\overline{e_n^2}$ are scattered and generally small enough not to affect $\overline{e_i^2}$ or $\overline{e^2}$. An exception is the $\omega_i = 2.5$ compensatory results, where a small value of $\overline{e_n^2}$ makes the $\overline{e^2}$ pursuit nearly equal to $\overline{e^2}$ compensatory.

$Y_c = K_c/s(s-\lambda)$ (Fig. 19)

Pursuit is increasingly better than compensatory as λ increases. This holds for both components of $\overline{e^2}$. Here $\overline{e_n^2}$ is on the order of $\overline{e_i^2}$.

$Y_c = K_c/s$ (Fig. 20)

Compensatory is slightly better at low and high bandwidth inputs for $\overline{e^2}$ with essentially no difference for moderate bandwidth inputs.

TABLE IV

SUMMARY OF PERFORMANCE MEASURE DIFFERENCES*

Y_c		FORCING FUNCTIONS				
		Augmented ω_i Spectra			Extended Band Spectra	
		1.5	2.5	4.0	B5	R14
K_c	$\overline{e^2}/\sigma_i^2$	P (0.76)	P (0.81)	P (0.80)	C (1.1)	Same
	$\overline{e_i^2}/\sigma_i^2$	P (0.79)	P (0.81)	P (0.76)	Same	Same
	$\overline{e_n^2}/\sigma_i^2$	P	PC	PC	C	CP
$\frac{K_c}{s^2}$	$\overline{e^2}/\sigma_i^2$	P (0.78)	P (0.95)	P (0.78)	P (0.81)	P (0.71)
	$\overline{e_i^2}/c_i^2$	PC (0.93)	P (0.89)	P (0.82)	P (0.72)	P (0.77)
	$\overline{e_n^2}/\sigma_i^2$	P	CP	P	Same	PC

Y_c		λ				
		0	0.5	1.0	1.5	
$\frac{K_c}{s(s-\lambda)}$	$\overline{e^2}/\sigma_i^2$	P (0.78)	P (0.71)	P (0.66)	P (0.59)	
	$\overline{e_i^2}/\sigma_i^2$	PC (0.93)	P (0.81)	P (0.61)	P (0.47)	
	$\overline{e_n^2}/\sigma_i^2$	P (0.65)	P (0.60)	P (0.72)	P (0.71)	

Y_c		FORCING FUNCTIONS				
		Augmented ω_i Spectra			Extended Band Spectra	
		1.5	2.5	4.0	B5	R14
$\frac{K_c}{s}$	$\overline{e^2}/\sigma_i^2$	CP (1.1)	C (1.27)	Same	Same	CP (1.07)
	$\overline{e_i^2}/\sigma_i^2$	C (1.2)	C (1.2)	CP	Same	P (0.87)
	$\overline{e_n^2}/\sigma_i^2$	P	C	Same	Same	C
$\frac{K_c(s+0.25)}{(s+5)^2}$	$\overline{e^2}/\sigma_i^2$	CP (1.05)	P (0.92)	Same		
	$\overline{e_i^2}/\sigma_i^2$	Same	P (0.91)	P (0.86)		
	$\overline{e_n^2}/\sigma_i^2$	CP	PC	C		

*Letters indicate configuration with lower measure, P (pursuit) or C (compensatory)
Numbers indicate relative rms performance measure

$Y_c = K_c(s+0.25)/(s+5)^2$ (Fig. 21)

For the bandwidths tested there is no significant difference between displays.

Thus, in general the performance improvement with pursuit display is largest for the more difficult controlled elements and inputs.

The mean-squared pilot output, $\overline{c^2}$, and its components, $\overline{c_i^2}$ and $\overline{c_n^2}$, are also shown in Figs. 17 – 21 . The $\overline{c^2}$ data show quite consistent trends, as does $\overline{c_i^2}$:

$Y_c = K_c$ (Fig. 17)

$\overline{c^2}$ and $\overline{c_i^2}$ are larger for pursuit display than for compensatory display. The increased pilot activity has resulted in less mean-squared error. $\overline{c^2}$ and $\overline{c_i^2}$ decrease as ω_i increases. $\overline{c_n^2}$ tends to increase as ω_i increases, but $\overline{c_n^2}$ is only in the order of 10 percent or less of $\overline{c^2}$ for the low frequency inputs, so the run-to-run variability of $\overline{c_n^2}$ doesn't mean much.

$Y_c = K_c/s^2$ and $K_c/s(s-\lambda)$ (Figs. 18 and 19)

$\overline{c^2}$ and $\overline{c_i^2}$ are lower for pursuit than for compensatory. Thus the improved performance ($\overline{e^2}$ and $\overline{e_i^2}$) is accomplished with less pilot activity. This contrasts with the case for $Y_c = K_c$ above. $\overline{c_n^2}$ is somewhat lower for pursuit for the augmented ω_i inputs, perhaps higher for B5 and R14.

$Y_c = K_c/s$ (Fig. 20)

$\overline{c_i^2}$ is lower for pursuit, whereas results for $\overline{c^2}$ are mixed. It appears that slightly better performance with the compensatory display is obtained with slightly higher effort.

$Y_c = K_c(s+0.25)/(s+5)^2$ (Fig. 21)

Results appear consistent. $\overline{c^2}$, $\overline{c_i^2}$, and $\overline{c_n^2}$ decrease (both for pursuit and compensatory) as ω_i increases. For $\overline{c^2}$ and $\overline{c_i^2}$ the trend appears to be that the operator works less with pursuit for $\omega_i = 1.5$, about the same for $\omega_i = 2.5$, and more for $\omega_i = 4.0$. These trends roughly parallel those for $\overline{e^2}$ and $\overline{e_i^2}$.

The mean-squared error and mean-squared pilot output results indicate that the pursuit display is desirable for the harder controlled elements, K_c/s^2 and $K_c/s(s-\lambda)$, in that the performance improves and less pilot activity is required. For $Y_c = K_c$ the pilot can also take advantage of the additional information presented, but he must use more activity to do so.

D. COMPARISON OF PURSUIT AND COMPENSATORY DESCRIBING FUNCTIONS

The describing function differences between the pursuit and compensatory displays are given in Figs. 22 – 26 in terms of the effective open-loop, Y_β (Eq. 11). Average data are shown with the range of the measurements indicated by the hatch marks. The pursuit data are plotted at the correct frequencies, while the compensatory data have been shifted slightly to the right. Detailed comparisons are:

$Y_c = K_c$ (Fig. 22)

For the augmented ω_i spectra the P has a slightly higher ω_c and low frequency gain which leads to less $\overline{e_i^2}$ (Fig. 17). For the B5 and R14 inputs, P has a slightly smaller ω_c but larger low frequency gain, such that $\overline{e_i^2}$ is about the same as C (Fig. 17). In general, P has more phase lag ($10^\circ - 30^\circ$) than C at mid-band

$Y_c = K_c/s^2$ (Fig. 23)

The most significant difference is the much smaller low frequency phase lag for P for all inputs. In addition, the P amplitude, which is nearly the same at low ω_i, becomes much smaller at mid-frequencies than the C as ω_i increases. Ordinarily this would lead to greatly increased $\overline{e_i^2}$ according to the one-third law approximation (Eq. 17). For this controlled element, phase lag has a large effect on $\overline{e_i^2}$ because the phase margin is small for C. Thus the increased phase margin for P has a larger effect on $\overline{e_i^2}$ than the reduced amplitude ratio.

$Y_c = K_c/s(s-\lambda)$ (Fig. 24)

The effect of the increasingly unstable controlled element (at $\omega_i = 1.5$ rad/sec) is a slightly smaller low frequency phase lag for P. For $\lambda = 1.5$ the P low frequency amplitude becomes

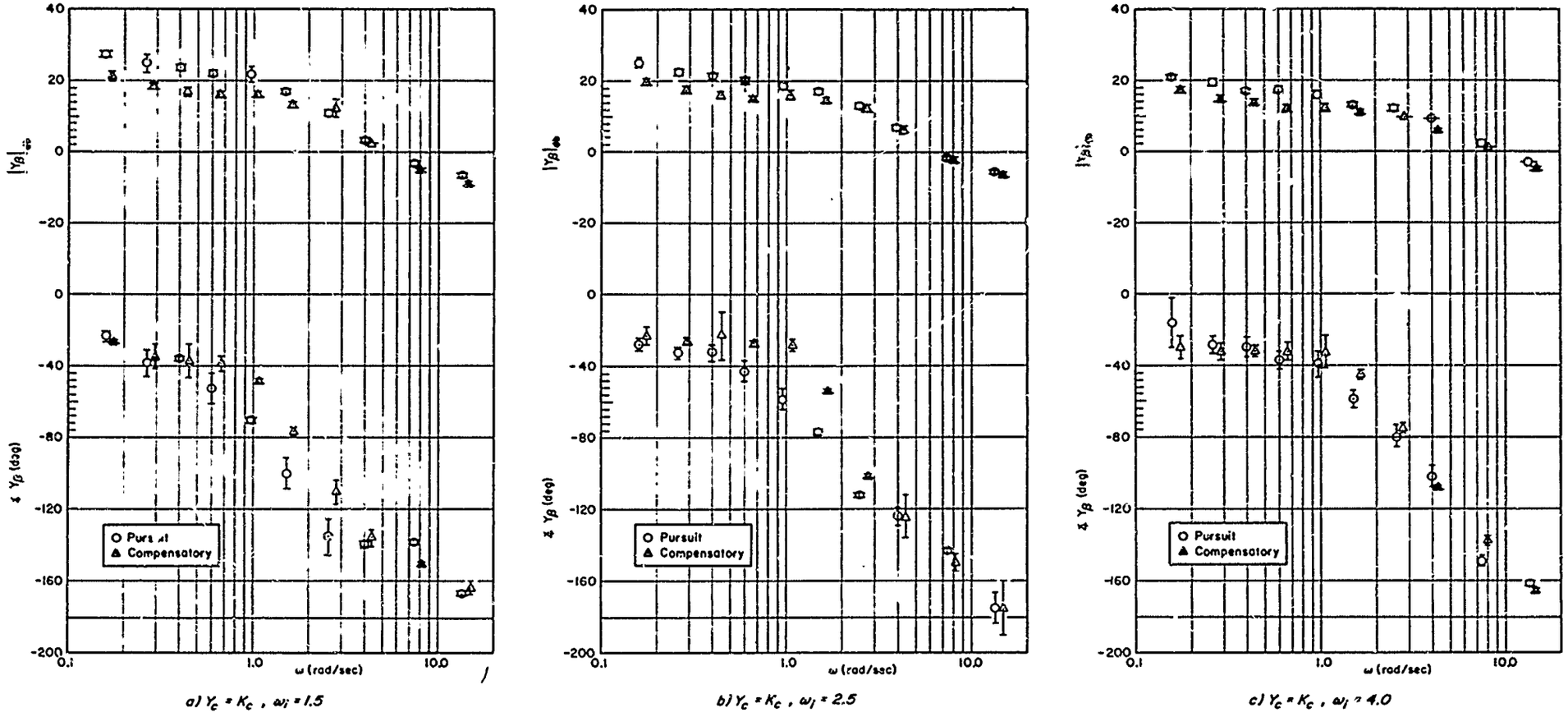

Figure 22. Comparison of Pursuit and Compensatory Display Describing Function

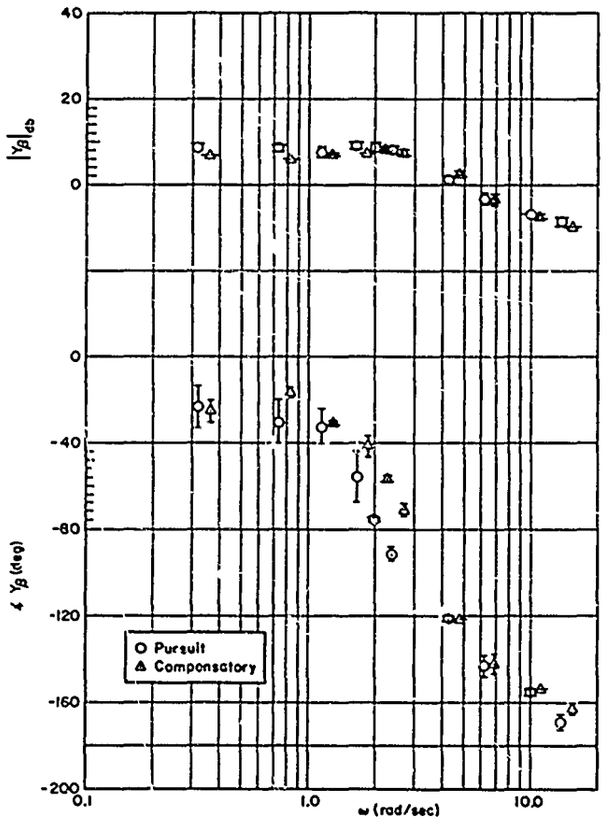

d) $Y_c = K_c$, B5 Input

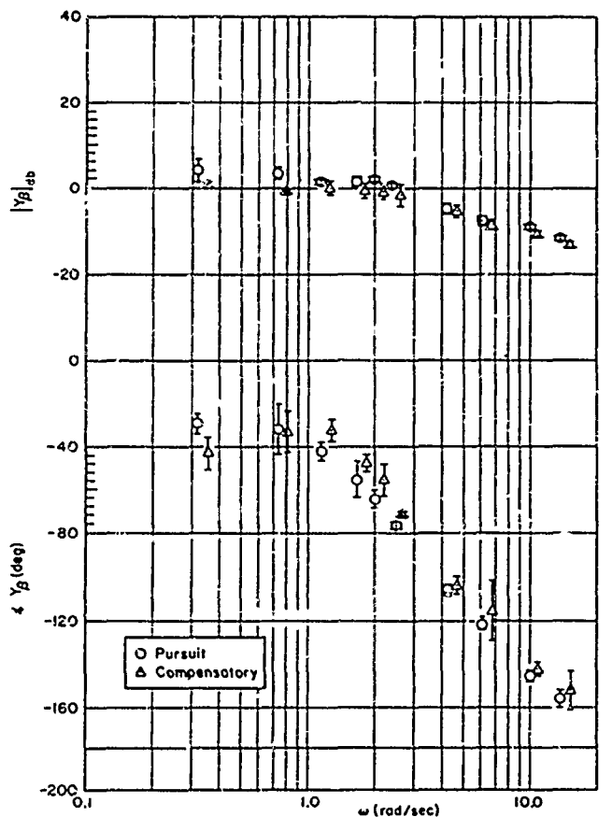

e) $Y_c = K_c$, R14 Input

Figure 22. (Concluded)

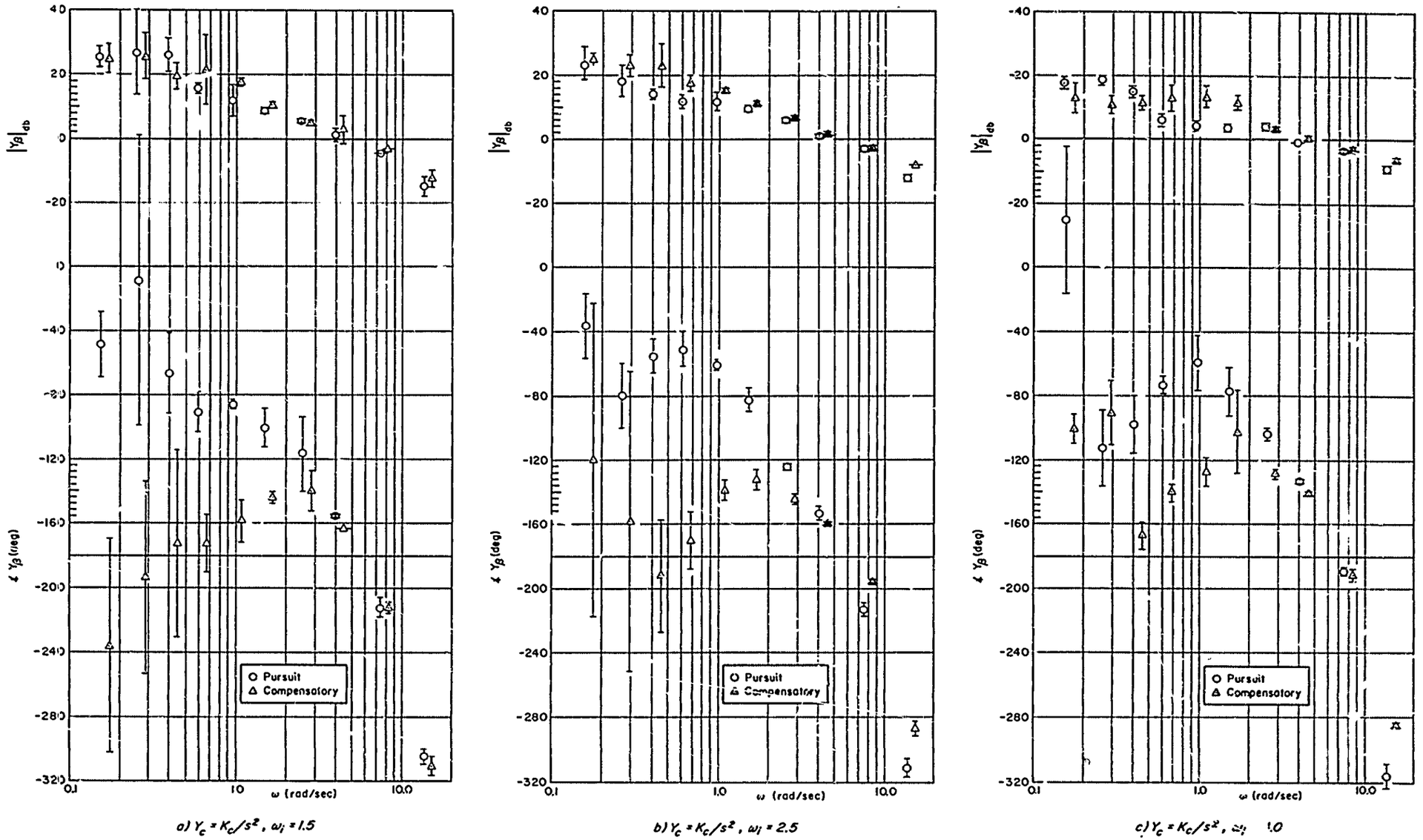

Figure 23. Comparison of Pursuit and Compensatory Display Describing Functions

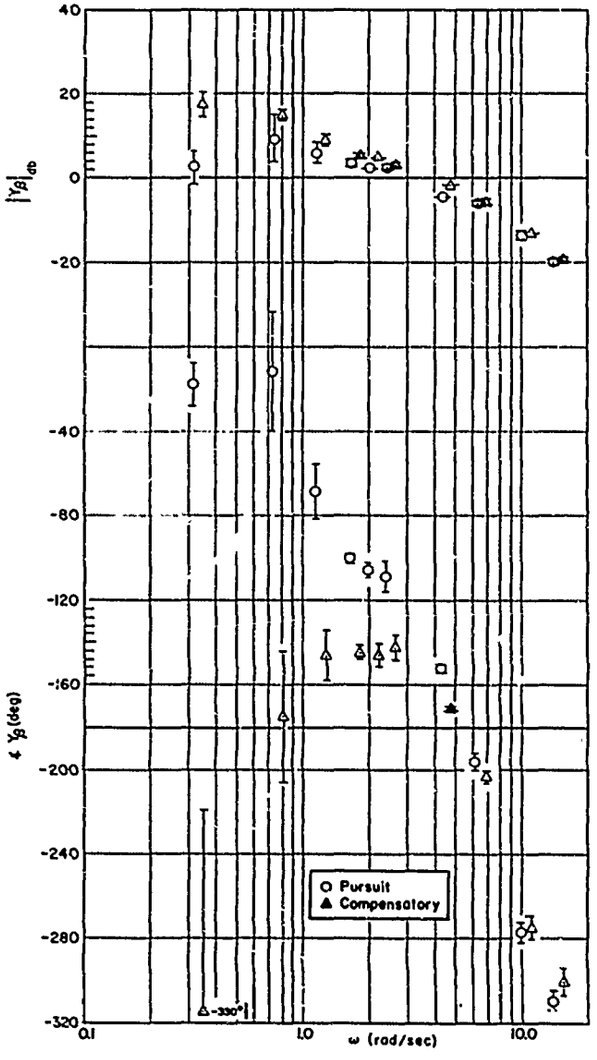

d) $Y_c = K_c/s^2$, B5 Input

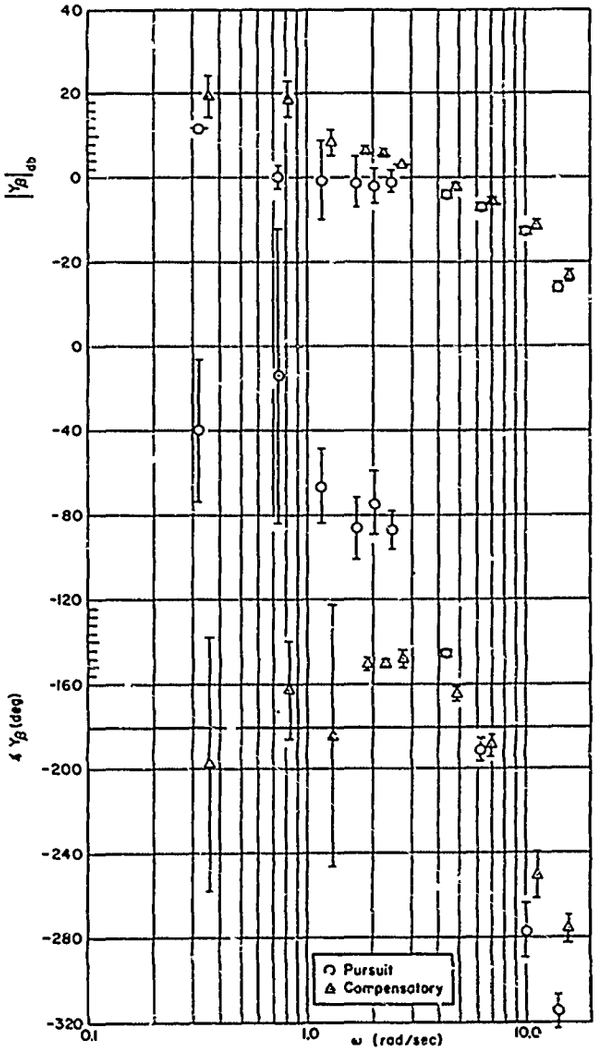

e) $Y_c = K_c/s^2$, R14 Input

Figure 23. (Concluded)

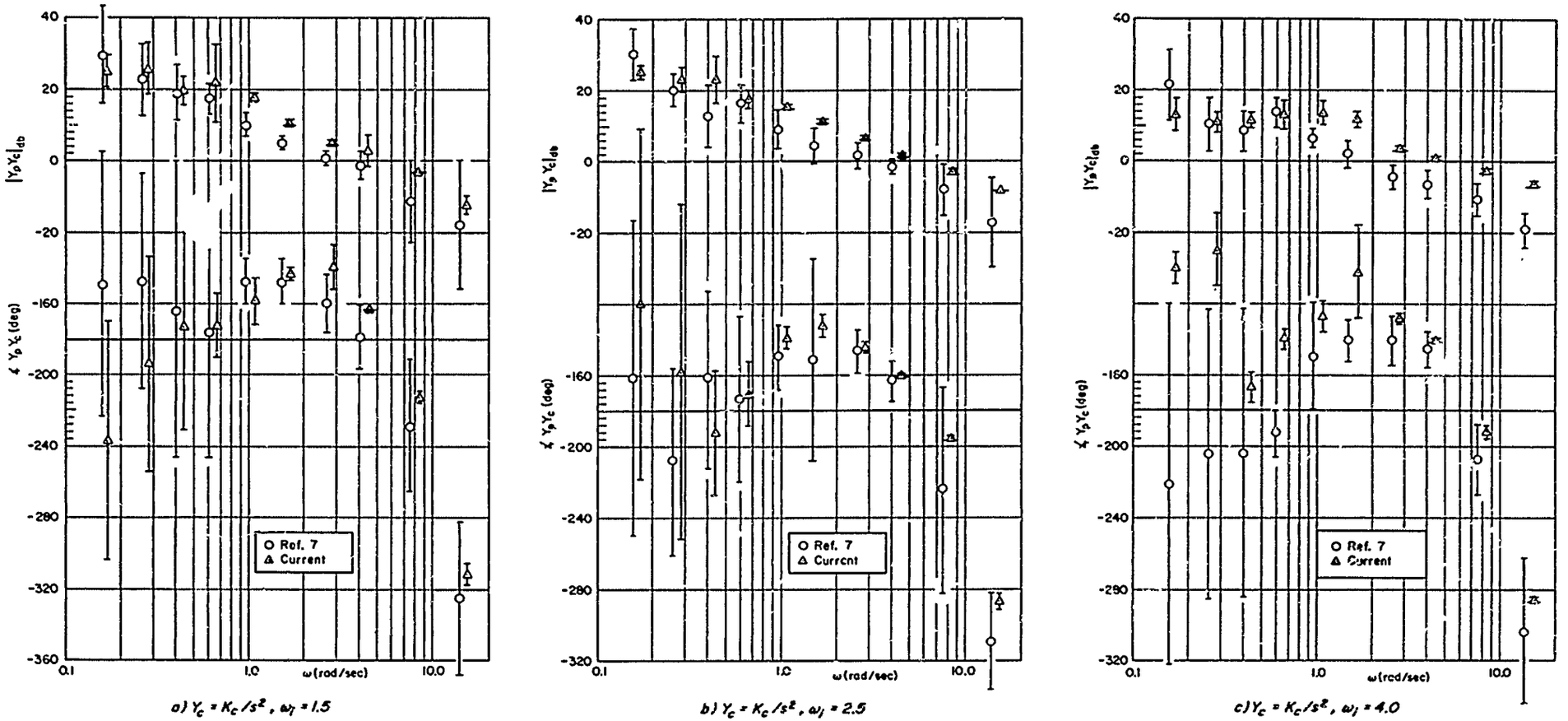

Figure 24. Comparison of Pursuit and Compensatory Display Describing Functions

slightly larger and the ω_c becomes slightly smaller than the C. Here, as for $Y_c = K_c/s^2$ above, the performance improvement is due mostly to the increased phase margin for the P.

$Y_c = K_c/s$ (Fig. 25)

For the lower ω_i's, P has slightly less amplitude at low frequency and at crossover leading to a larger $\overline{e_i^2}$ (Fig. 20). The same amplitude trends hold for the B5 input but now the P has slightly less phase lag, such that $\overline{e_i^2}$ shows no difference. For the R14 input the P amplitude ratio is much smaller and there is less phase lag, leading to an improvement in $\overline{e_i^2}$ (Fig. 20).

$Y_c = K_c(s+0.25)/(s+5)^2$ (Fig. 26)

Very little difference between P and C.

Thus, the describing function and performance measure comparisons indicate that the pursuit display is superior to the compensatory display for $Y_c = K_c$, K_c/s^2, and $K_c/s(s-\lambda)$. For $Y_c = K_c$ the subject improves performance by increasing the bandwidth of the effective open-loop, Y_β, but must increase his activity slightly. For $Y_c = K_c/s^2$ and $K_c/s(s-\lambda)$ performance improvements are obtained by drastic changes in the phase of Y_β but with less pilot activity.

Figure 24. Comparison of Pursuit and Compensatory Display Describing Functions

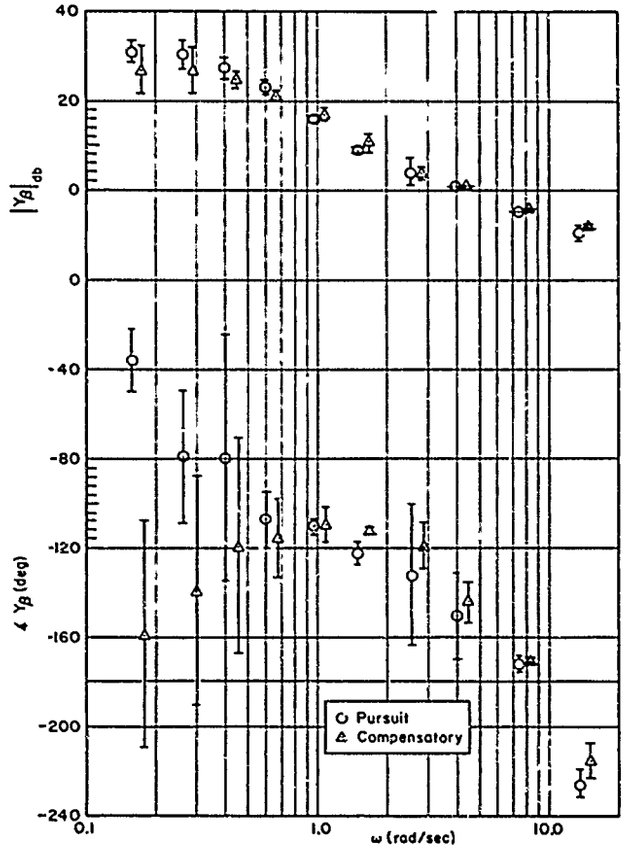

a) $Y_c = K_c/s$, $\omega_l = 1.5$

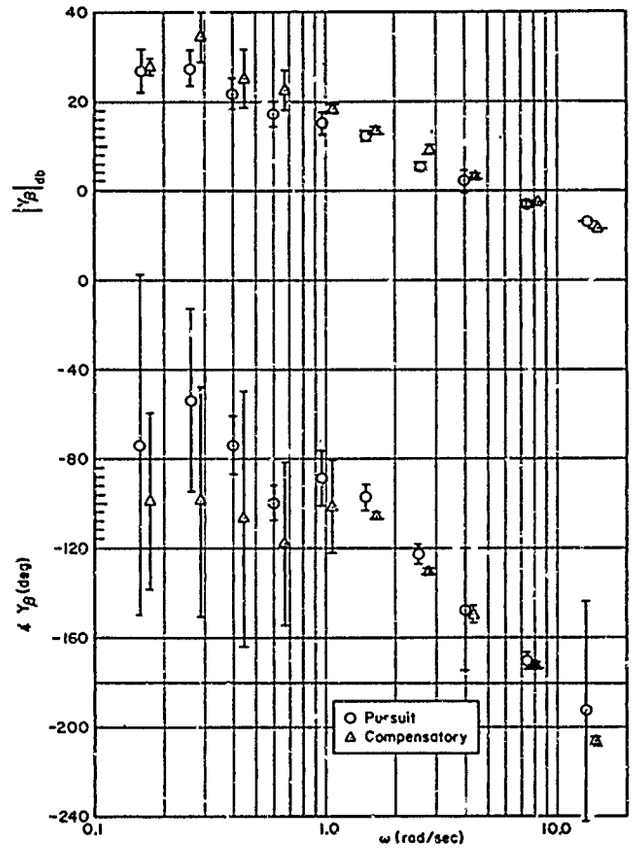

b) $Y_c = K_c/s$, $\omega_l = 2.5$

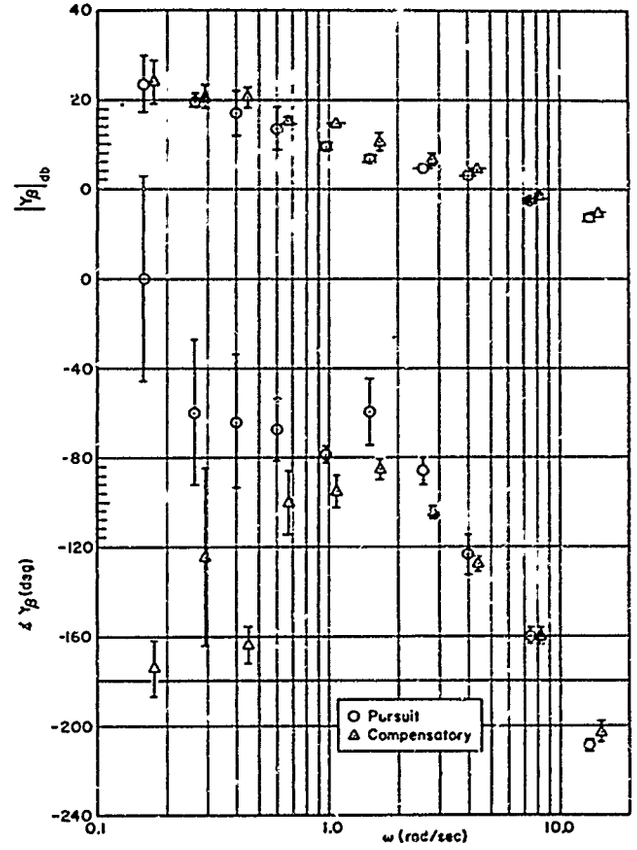

c) $Y_c = K_c/s$, $\omega_l = 4.0$

Figure 25. Comparison of Pursuit and Compensatory Display Describing Functions

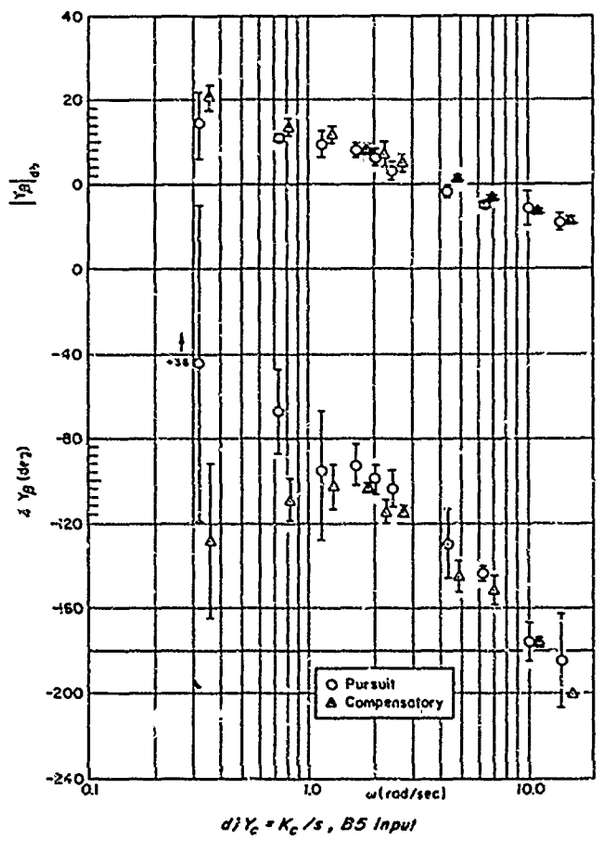

d) $Y_c = K_c/s$, B5 Input

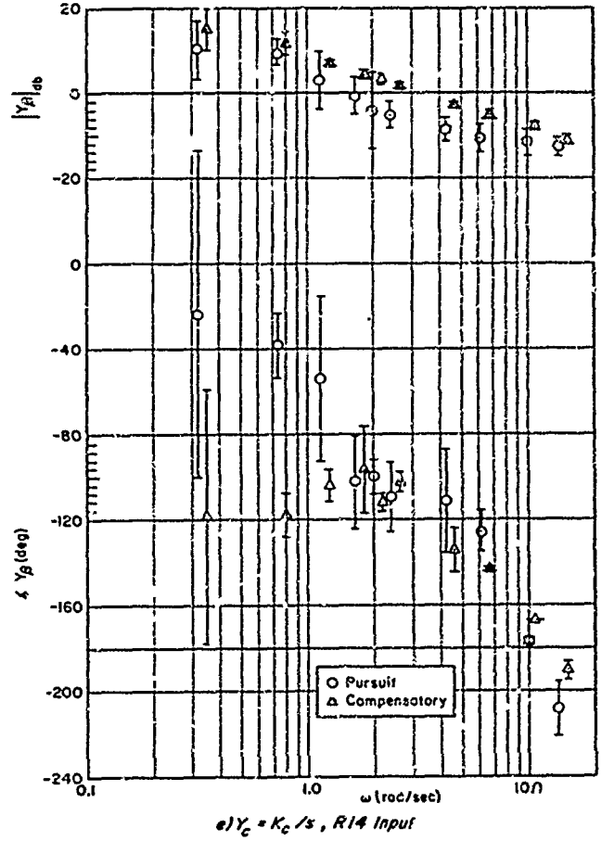

e) $Y_c = K_c/s$, R14 Input

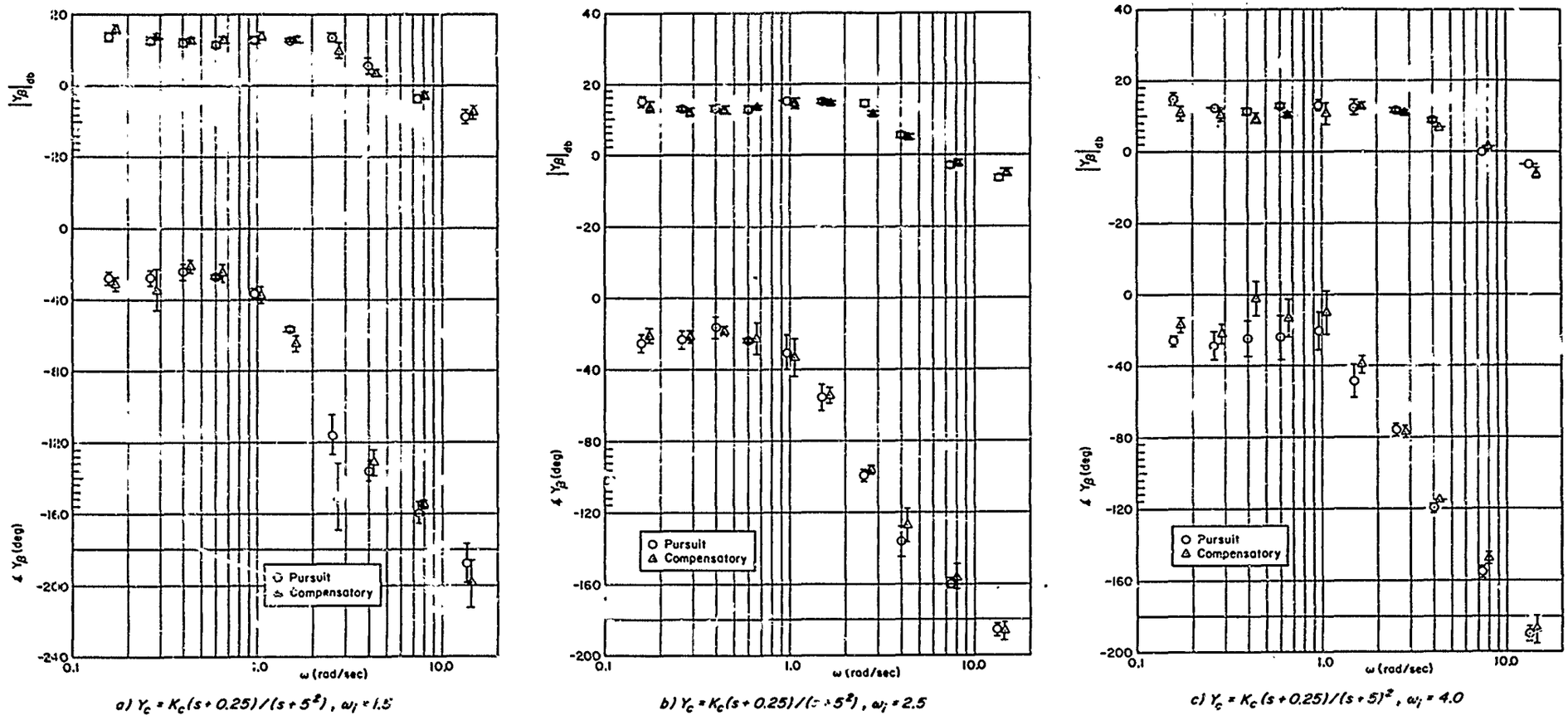

Figure 26. Comparison of Pursuit and Compensatory Display Describing Functions

CHAPTER V

DATA INTERPRETATION

The data in the previous chapter indicate the differences between pursuit and compensatory display situations. The purpose of this chapter is to interpret the data as to the possible nature of the pilot's organization. As indicated in Chapter III, the explicit determination of the pilot's describing functions is not possible with a single forcing function. Nevertheless, using reasonable assumptions it is possible to imply certain characteristics about the pilot's operation in system stabilization as well as his operation on the input.

The discussion in Chapter III indicates that only two of the pilot's describing functions (Y_{p_i}, Y_{p_e} and Y_{p_m}) are independent, i.e., any box can be zero and the other two can describe the data. Of the three possibilities, we will assume that $Y_{p_m} = 0$.* The pursuit situation then becomes as in Fig. 27, where the system error and output spectra are, from Eqs. 6 and 7 with $Y_{p_m} = 0$

$$\Phi_{mm} = \left|\frac{\left(Y_{p_i} + Y_{p_e}\right)Y_c}{1 + Y_{p_e}Y_c}\right|^2 \Phi_{ii} + \left|\frac{Y_c}{1 + Y_{p_e}Y_c}\right|^2 \Phi_{n_c n_c} \qquad (20)$$

$$\Phi_{ee} = \left|\frac{1 - Y_c Y_{p_i}}{1 + Y_{p_e}Y_c}\right|^2 \Phi_{ii} + \left|\frac{Y_c}{1 + Y_{p_e}Y_c}\right|^2 \Phi_{n_c n_c} \qquad (21)$$

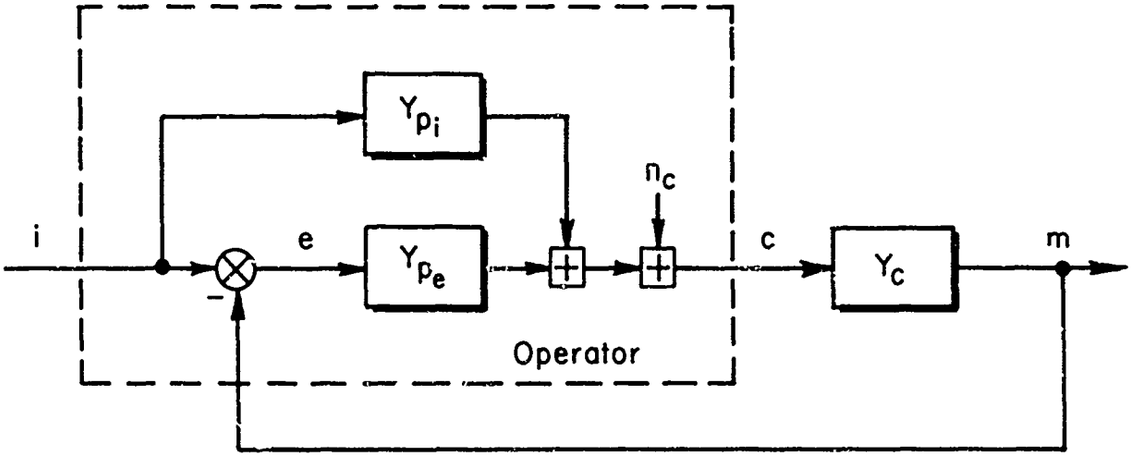

Figure 27. Single-Axis Pursuit Tracking

*The data were also examined using the assumption that $Y_{p_i} = 0$ thereby leaving Y_{p_e} and Y_{p_m} to describe the pilot's behavior. However, this approach did not result in any useful interpretation of the data.

Since system stability and low frequency error reduction are determined by Y_{p_e}, an appropriate model for the pilot to adopt is that which results for the same controlled element in the compensatory situation, i.e.,

$$Y_{p_e} = Y_{p_c} \tag{22}$$

If Y_{p_i} is selected so that

$$Y_{p_i} Y_c \doteq 1 \tag{23}$$

then the system output (neglecting the remnant) approximately equals the input resulting in smaller error. Thus, the pilot can take advantage of the additional information in the pursuit display by adopting equalization that is the inverse of the controlled element. The system then becomes nearly open-loop through the feedforward, with the feedback acting as a vernier control and as a means of stabilizing the controlled element.

To test this hypothesis an implied feedforward, $Y^*_{p_i}$, can be calculated from the assumption that Y_{p_e} for the pursuit display is the same as the measured Y_{p_c} for the corresponding compensatory display. Thus, Eq. 11, repeated below, can be solved for $Y^*_{p_i}$ on the assumption that $Y_{p_e} = Y_{p_c}$ and that $Y_{p_m} = 0$.

$$Y_\beta = \frac{\Phi_{im}}{\Phi_{ie}} = \frac{\left(Y^*_{p_i} + Y_{p_c}\right) Y_c}{1 - Y^*_{p_i} Y_c} \tag{24}$$

Solving for $Y^*_{p_i} Y_c$ yields

$$Y^*_{p_i} Y_c = \frac{Y_\beta - Y_c Y_{p_c}}{1 + Y_\beta} \tag{25}$$

The implied feedforward was calculated using averaged data for Y_β and Y_{p_c}. The results are given in Figs. 28–30 for the cases that showed large performance differences, i.e., $Y_c = K_c$, K_c/s^2, $K_c/s(s - \lambda)$, respectively. The results are given in $Y^*_{p_i} Y_c$ form to illustrate the extent that the ideal adjustment given by Eq. 23, in the light of the assumption given by Eq. 22, is approached. Detailed comments are:

$Y_c = K_c$ (Fig. 28)

$Y^*_{p_i} Y_c$ is less than one and approximately constant, but with lagging phase at high frequency similar to that of a time delay.

$Y_c = K_c/s^2$ (Fig. 29)

$Y^*_{p_i} Y_c$ is greater than one at low frequency, then becomes much less than one at high frequencies. The phase is positive ($20^\circ - 60^\circ$) at low band and mid-band frequencies becoming negative at high frequency.

$Y_c = K_c/s(s-\lambda)$ (Fig. 30)

Generally $Y^*_{p_i} Y_c$ stays closer to unity at all frequencies than for $Y_c = K_c/s^2$, although the general character is the same. As λ increases, $Y^*_{p_i} Y_c$ becomes closer to unity, reflecting the relative reduction in performance measures (Fig. 19).

For the second-order controlled elements additional dynamics are present. These are partially obscured by data scatter at low frequencies probably due to taking differences between large numbers (numerator of Eq. 25). Nevertheless, the pilot appears to be able to invert the controlled element at low frequencies up to just below crossover.

For the single-forcing-function case, the advantages of the above assumptions and procedures are:

- The division of the pilot's actions cannot be unique, so any combination of Y_{p_i}, Y_{p_e}, Y_{p_m} compatible with the data is equally appropriate on theoretical grounds.
- The pilot adjustment rules for the compensatory situation (Ref. 7) can be utilized for Y_{p_c}, and a first-cut estimate for Y_{p_i} can be made on the basis of Y_c.

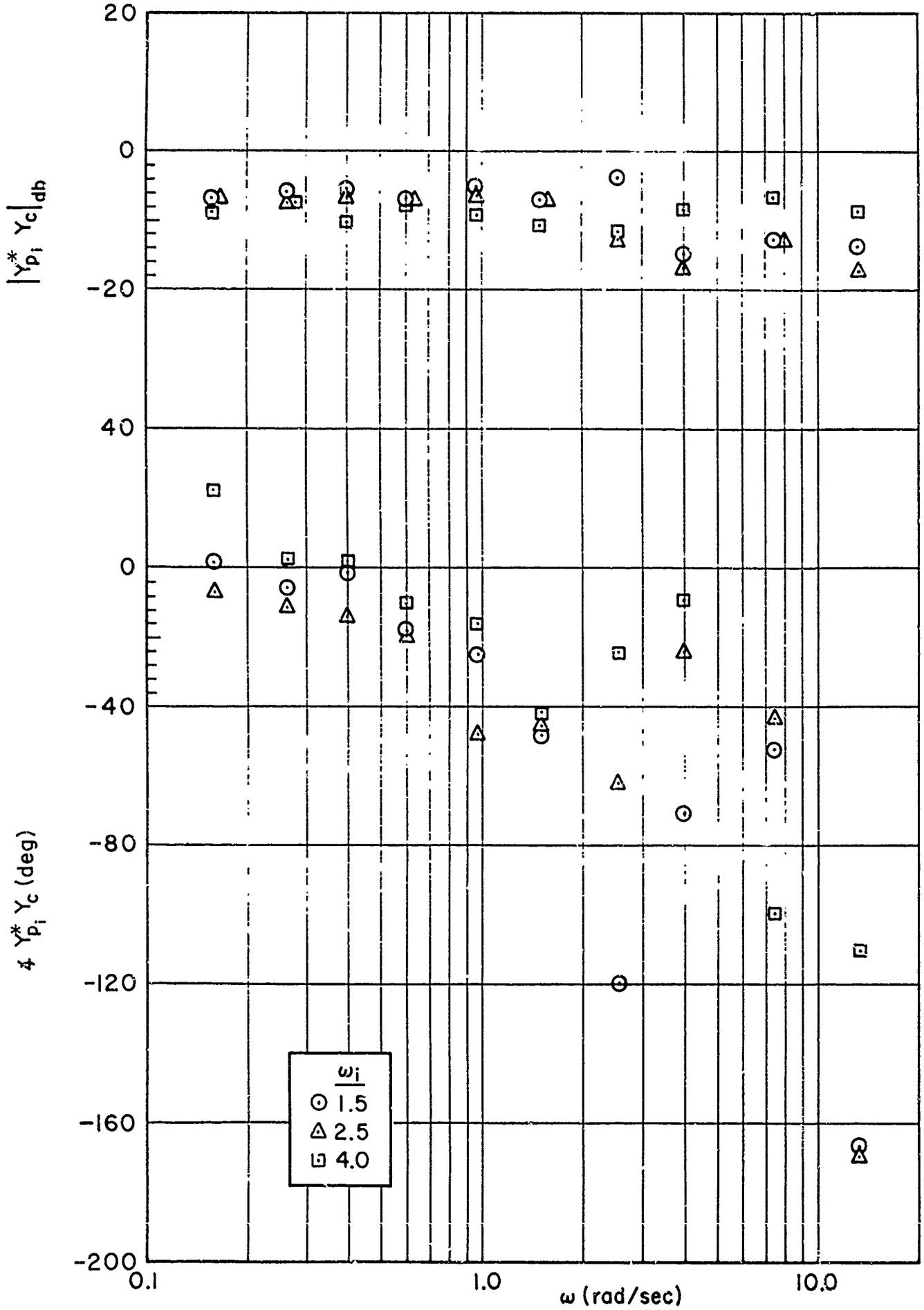

Figure 28. Implied Human Operator Feedforward Characteristics, $Y_c = K_c$

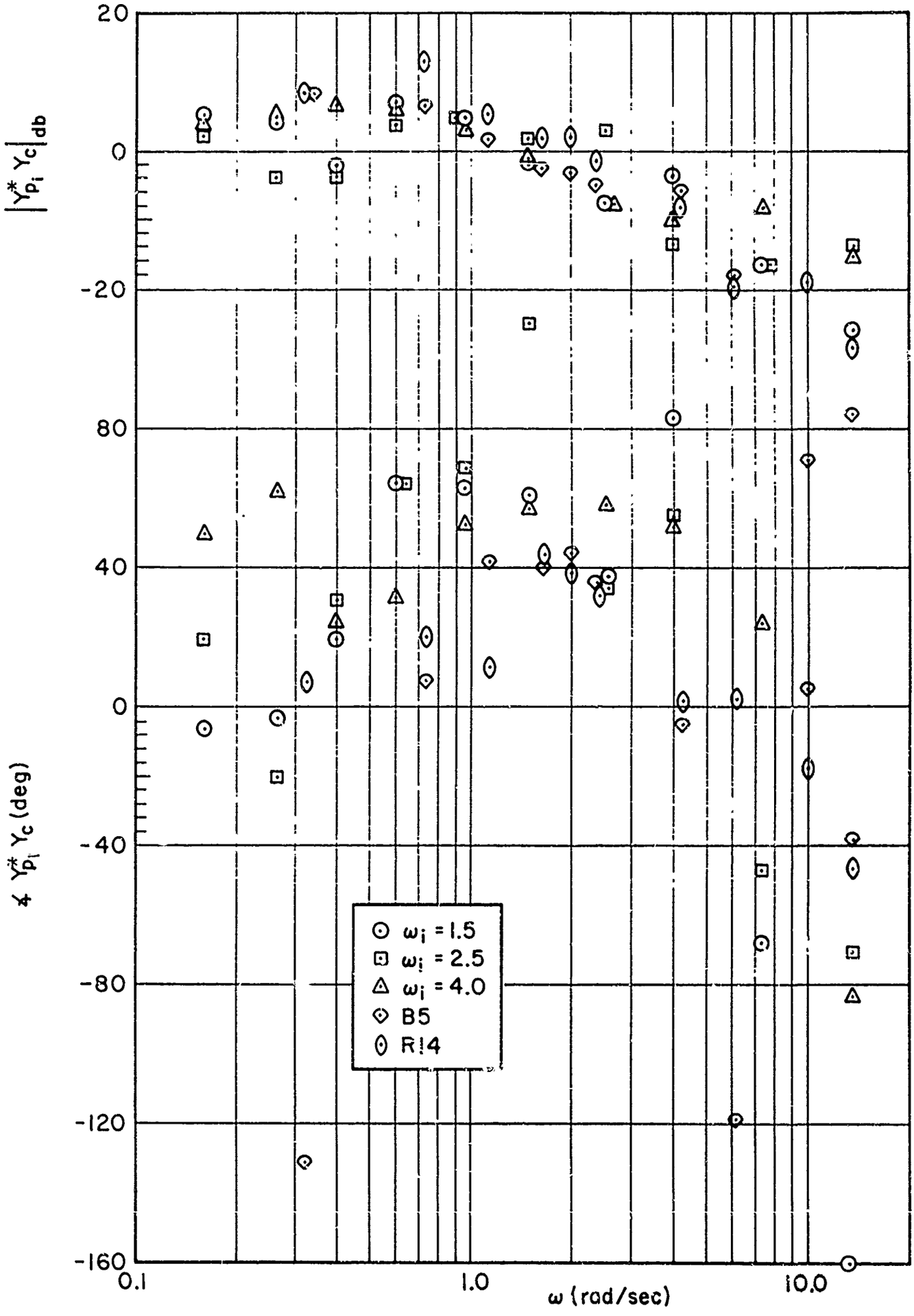

Figure 29. Implied Human Operator Feedforward Characteristics, $Y_c = K_c/s^2$

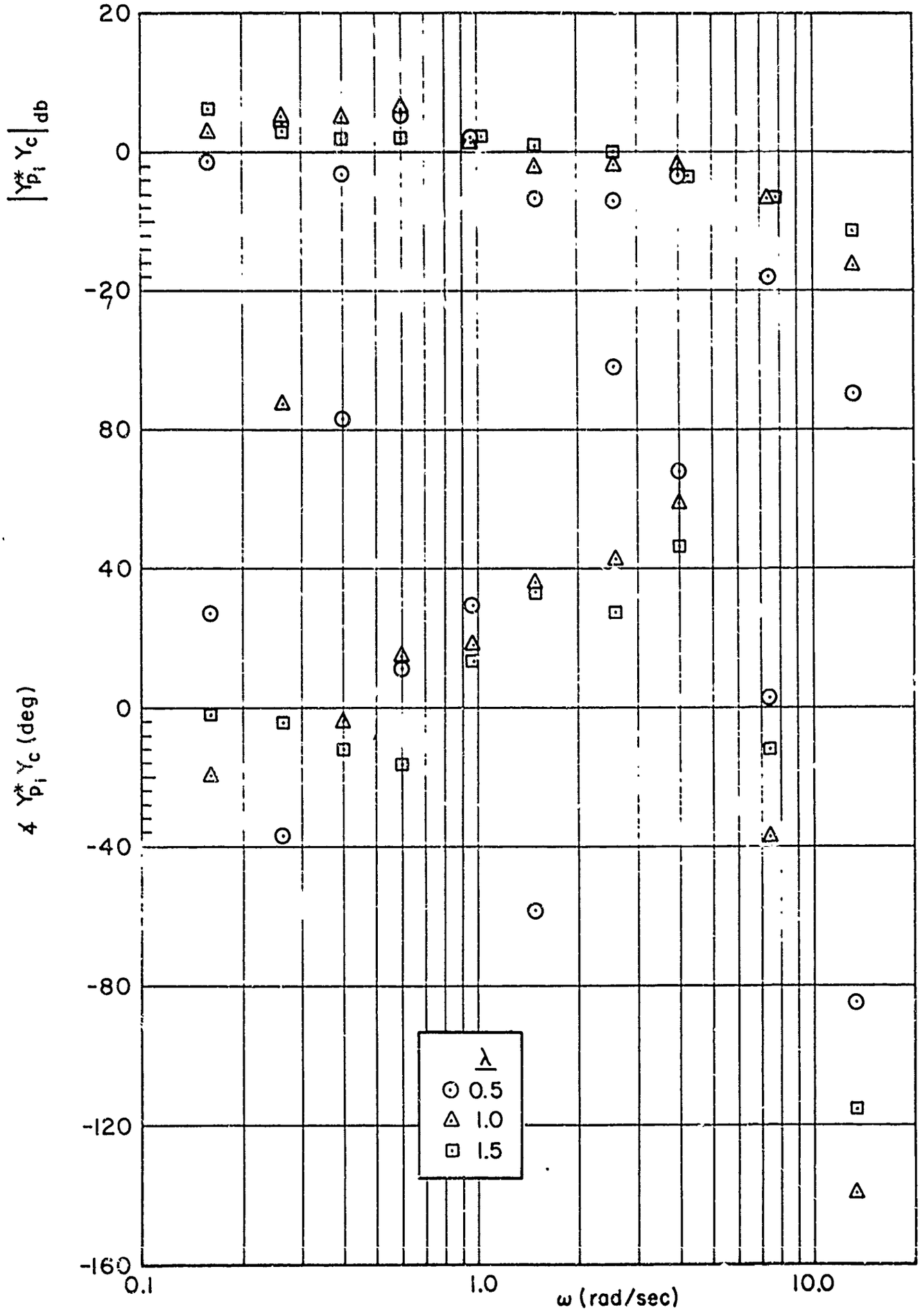

Figure 30. Implied Human Operator Feedforward Characteristics
$Y_c = K_c/s(s-\lambda)$, $\omega_1 = 1.5$

CHAPTER VI

GENERAL CONCLUSIONS

The data and analyses presented in this report indicate many differences between pursuit and compensatory systems. Unfortunately, many of these distinctions are subtle and the ones that are clear-cut are not general. Most of these features have been described in the local discussions of the data and need not be repeated here. The broader and more general conclusions are, however, summarized below:

1. The describing function data and performance measure trends for the $Y_c = K_c$ series correspond very well with those of a previous investigation by Elkind.

2. The compensatory describing function data for the series reported here tie in fairly well with an earlier series in which the present subject was but one member of a population.

3. A sufficient indication of pursuit behavior is that Y_β-pursuit differs from Y_β-compensatory.

4. The operator dynamics as measured by the effective open-loop describing function, Y_β, are different for all but one of the controlled-element/forcing-function combinations tested. Thus, in all but the exceptional case the presence of the pursuit display is sufficient to induce pursuit behavior.

5. The provision of a pursuit display does not necessarily induce pursuit behavior. This is shown conclusively for $Y_c = K_c(s+0.25)/(s+5)^2$, for which Y_β is the same in the pursuit and compensatory conditions.

6. For those systems where pursuit and compensatory dynamic differences were present, in three cases [K_c, K_c/s^2, and $K_c/s(s-\lambda)$] pursuit was superior and in one case (K_c/s) compensatory was better.

7. For the augmented ω_1 spectra the normalized mean-squared errors are smaller for pursuit display in all cases where Y_β-pursuit is superior to Y_β-compensatory.

8. The relative superiority of pursuit over compensatory, when present, increases as the controlled element becomes more difficult to control, i.e., higher bandwidths or larger instabilities.

9. The differences between pursuit and compensatory behavior are often subtle and confusing. A plausible description

of pursuit operations is:

> The compensatory loop portion of the pursuit system has dynamics similar to those of the corresponding compensatory system. Thus the analytical/verbal model for compensatory operation can be applied to pursuit.
>
> When pursuit behavior is actually present the pilot operates directly on the forcing function, thereby adding an additional describing function block, Y_{p_i}, to the system structure. To a first approximation the feedforward, Y_{p_i}, is adjusted such that $|Y_{p_i}Y_c| \doteq 1$. Such adjustment has the net effect of making $M/T \doteq 1$ and $E/I \doteq 0$ over a wide frequency band.

This model for pursuit action is not a unique description of pursuit operation, although it becomes so when the constraint is applied that the compensatory portion of the pursuit system will be the same as that measured for the compensatory display.

REFERENCES

1. Chernikoff, Rube, Henry P. Birmingham, and Franklin V. Taylor, "A Comparison of Pursuit and Compensatory Tracking Under Conditions of Aiding and No Aiding," J. Exp. Psychol., Vol. 49, No. 1, 1955, pp. 55-59.

2. Chernikoff, Rube, and Franklin V. Taylor, "Effects of Course Frequency and Aided Time Constant on Pursuit and Compensatory Tracking," J. Exp. Psychol., Vol. 53, No. 5, 1957, pp. 285-292.

3. Elkind, Jerome I., Characteristics of Simple Manual Control Systems, MIT Lincoln Lab. Tech. Rept. 111, 6 Apr. 1956.

4. Hartman, Bryce O., The Effect of Target Frequency on Compensatory Tracking, U. S. Army Medical Research Lab. Rept. 272, 25 Apr. 1957.

5. Hartman, Bryce O., The Effect of Target Frequency on Pursuit Tracking, U. S. Army Medical Research Lab. Rept. 263, 20 Mar. 1957.

6. Krendel, Ezra S., and Duane T. McRuer, "A Servomechanisms Approach to Skill Development," J. Franklin Inst., Vol. 269, No. 1, Jan. 1960, pp. 24-42.

7. McRuer, Duane, Dunstan Graham, Ezra Krendel, and William Reisener, Jr., Human Pilot Dynamics in Compensatory Systems — Theory, Models, and Experiments with Controlled Element and Forcing Function Variations, AFFDL-TR-65-15, Jan. 1965.

8. McRuer, D. T., and E. S. Krendel, Dynamic Response of Human Operators, WADC-TR-56-524, Oct. 1957.

9. Obermayer, R. W., W. F. Swartz, and F. A. Muckler, "Interaction of Information Displays with Control System Dynamics and Course Frequency in Continuous Tracking," Perceptual and Motor Skills, Vol. 15, No. 1, Aug. 1962, pp. 199-215.

10. Poulton, E. C., "Perceptual Anticipation in Tracking with Two-Pointer and One-Pointer Displays," British J. Psychol., Vol. 43, 1952, pp. 222-229.

11. Senders, John W., and Marianne Cruzen, Tracking Performance on Combined Compensatory and Pursuit Tasks, WADC-TR-52-39, Feb. 1952.

12. Walston, C. E., and C. E. Warren, A Mathematical Analysis of the Human Operator in a Closed-Loop Control System, AFPTRC-TR-54-96, 1954.

Unclassified

Security Classification

DOCUMENT CONTROL DATA - R&D

(Security classification of title, body of abstract and indexing annotation must be entered when the overall report is classified)

1 ORIGINATING ACTIVITY (Corporate author) STI 13766 S. Hawthorne Boulevard Hawthorne, California 90250	2a. REPORT SECURITY CLASSIFICATION Unclassified 2b GROUP N/A

3. REPORT TITLE

Human Pilot Dynamic Response In Single-Loop Systems With Compensatory And Pursuit Displays

4 DESCRIPTIVE NOTES *(Type of report and inclusive dates)*

Final Technical Report

5. AUTHOR(S) *(Last name, first name, initial)*

Wasicko, R. J.
McRuer, D. T.
Magdaleno, R. E.

6. REPORT DATE	7a TOTAL NO. OF PAGES	7b. NO. OF REFS
December 1966	84	12

8a. CONTRACT OR GRANT NO.	9a. ORIGINATOR'S REPORT NUMBER(S)
AF 33(657)-10835 b. PROJECT NO. 8219 c. Task: 821905 d.	AFFDL-TR-66-137 9b. OTHER REPORT NO(S) *(Any other numbers that may be assigned this report)* STI-TR-134-4

10

Distribution of this document is unlimited.

11. SUPPLEMENTARY NOTES	12. SPONSORING MILITARY ACTIVITY
	AFFDL (FDCC) Wright-Patterson AFB, Ohio 45433

13. ABSTRACT

The primary purpose of the experimental series reported here is to investigate, on a preliminary and exploratory basis, human operator performance differences between pursuit and compensatory displays. For each display type a wide range of forcing function bandwidths and controlled element dynamics was used. The effect of the additional information provided by separately displaying both forcing function and controlled element output (pursuit) rather than their difference (compensatory) was evaluated using the mean-squared error and a quantity called the "effective open-loop describing function" (Y_e).

As a prelude to the new data, past pursuit/compensatory tracking results are reviewed, and then a tie-in is made between these and the current series.

DD FORM 1 JAN 64 1473

Unclassified

Security Classification

14. KEY WORDS	LINK A		LINK B		LINK C	
	ROLE	WT	ROLE	WT	ROLE	WT
Human Response Pursuit Display Human Engineering Flight Control Systems Pilot Models						

INSTRUCTIONS

1. ORIGINATING ACTIVITY: Enter the name and address of the contractor, subcontractor, grantee, Department of Defense activity or other organization *(corporate author)* issuing the report.

2a. REPORT SECURITY CLASSIFICATION: Enter the overall security classification of the report. Indicate whether "Restricted Data" is included. Marking is to be in accordance with appropriate security regulations.

2b. GROUP: Automatic downgrading is specified in DoD Directive 5200.10 and Armed Forces Industrial Manual. Enter the group number. Also, when applicable, show that optional markings have been used for Group 3 and Group 4 as authorized.

3. REPORT TITLE: Enter the complete report title in all capital letters. Titles in all cases should be unclassified. If a meaningful title cannot be selected without classification, show title classification in all capitals in parenthesis immediately following the title.

4. DESCRIPTIVE NOTES: If appropriate, enter the type of report, e.g., interim, progress, summary, annual, or final. Give the inclusive dates when a specific reporting period is covered.

5. AUTHOR(S): Enter the name(s) of author(s) as shown on or in the report. Enter last name, first name, middle initial. If military, show rank and branch of service. The name of the principal author is an absolute minimum requirement.

6. REPORT DATE: Enter the date of the report as day, month, year; or month, year. If more than one date appears on the report, use date of publication.

7a. TOTAL NUMBER OF PAGES: The total page count should follow normal pagination procedures, i.e., enter the number of pages containing information.

7b. NUMBER OF REFERENCES: Enter the total number of references cited in the report.

8a. CONTRACT OR GRANT NUMBER: If appropriate, enter the applicable number of the contract or grant under which the report was written.

8b, 8c, & 8d. PROJECT NUMBER: Enter the appropriate military department identification, such as project number, subproject number, system numbers, task number, etc.

9a. ORIGINATOR'S REPORT NUMBER(S): Enter the official report number by which the document will be identified and controlled by the originating activity. This number must be unique to this report.

9b. OTHER REPORT NUMBER(S). If the report has been assigned any other report numbers *(either by the originator or by the sponsor)*, also enter this number(s).

10. AVAILABILITY/LIMITATION NOTICES: Enter any limitations on further dissemination of the report, other than those imposed by security classification, using standard statements such as:

(1) "Qualified requesters may obtain copies of this report from DDC."

(2) "Foreign announcement and dissemination of this report by DDC is not authorized."

(3) "U. S. Government agencies may obtain copies of this report directly from DDC. Other qualified DDC users shall request through

_____."

(4) "U. S. military agencies may obtain copies of this report directly from DDC. Other qualified users shall request through

_____."

(5) "All distribution of this report is controlled. Qualified DDC users shall request through

_____."

If the report has been furnished to the Office of Technical Services, Department of Commerce, for sale to the public, indicate this fact and enter the price, if known.

11. SUPPLEMENTARY NOTES: Use for additional explanatory notes.

12. SPONSORING MILITARY ACTIVITY: Enter the name of the departmental project office or laboratory sponsoring *(paying for)* the research and development. Include address.

13 ABSTRACT: Enter an abstract giving a brief and factual summary of the document indicative of the report, even though it may also appear elsewhere in the body of the technical report. If additional space is required, a continuation sheet shall be attached.

It is highly desirable that the abstract of classified reports be unclassified. Each paragraph of the abstract shall end with an indication of the military security classification of the information in the paragraph, represented as *(TS), (S), (C), or (U)*.

There is no limitation on the length of the abstract. However, the suggested length is from 150 to 225 words.

14 KEY WORDS: Key words are technically meaningful terms or short phrases that characterize a report and may be used as index entries for cataloging the report. Key words must be selected so that no security classification is required. Identifiers, such as equipment model designation, trade name, military project code name, geographic location, may be used as key words but will be followed by an indication of technical context. The assignment of links, rules, and weights is optional.

AFFDL-TR-66-137

AD-646652

ERRATA

The data plots and controlled element designations on p. 29 should be interchanged with that on p. 52.